Liquid Metal-Air Battery for Energy Storage

A Major Qualifying Project Report submitted to the Faculty of the
WORCESTER POLYTECHNIC INSTITUTE
Chemical Engineering Department
in partial fulfillment of the requirements for the
Degree of Bachelor of Science

Submitted by

Victor Hu

Huyen Vu

Jacob Zagorski

Date: April 28, 2016

Adviser: Ravindra Datta

Abstract

As the energy demand increases with a growing population and standards of living, more renewable energy will be incorporated into the grid to minimize the needs for fossil fuels, a finite resource. Due to the intermittent power generation of wind and solar energy, energy storage is required to store and release excess energy when needed. Liquid metal-air flow batteries show potential for grid-scale storage due to their high theoretical energy densities and long durations. Improvements were made to a previous design of a gallium-air battery that greatly extended its discharge period to more than 25 hours. However, the battery still suffers from electrolyte evaporation and carbonation that limits duration. Flow batteries are possible based on this design with electrolyte replenishment.

Acknowledgement

This research was supported by the Department of Chemical Engineering at Worcester Polytechnic Institute. A special thanks to last year's *A New Liquid Metal-Air* Battery MQP group for providing the majority of the equipment and supplies along with providing their expertise and insights in the research.

We would also like to show our appreciation to Thomas Partington and Douglas White for their assistance with electrical and mechanical components for the research. Their skills and expertise in the field provided us the tools that we needed to conduct this project.

Most importantly, we would like to thank our advisor, Professor Ravindra Datta, for advising us throughout this project. His support and wisdom helped guide our project to where it is today.

TABLE OF CONTENTS

TABLE OF FIGURES

TABLE OF TABLES

CHAPTER 1: INTRODUCTION

Energy storage is an important aspect of the global economy as the consumption of energy soars. By 2040, global consumption of energy is predicted to increase by 37 percent (IAE, 2014). Fossil fuels have been the primary supplier for the needed energy, but are a limited source. They also present environmental risks and hazards, as they are a prominent source of excess carbon dioxide and other greenhouse gases emitted into the atmosphere (Bouhafs, et al. 2014). Another critical factor concerns fossil fuel dependence, since the United States currently imports a majority of their oil. As a result, many states are mandating renewable portfolios to expedite the integration and implementation of cleaner, more renewable energy sources (Eastin, 2014). With each successive year, the pace of this integration continues to rise and is expected to continue as the capital costs of wind and solar power decline.

As the generation of renewable energy increases, so does the need for a more efficient power grid that incorporate more advanced energy storage systems. Although wind and solar energy can produce a lot of electricity, the problem they both face is intermittent power generation. Wind performance depends on the wind speed throughout the day, which can fluctuate unpredictably at times and with seasons. As for solar energy, the production peaks around noon time and ceases to exist at night time, weather permitting. The energy demand within a day fluctuates, but is highest at late evening. Unfortunately, that high demand does not always correspond with peak renewable energy production, so fossil fuels are still utilized to make up the difference. Ideally, using energy storage would allow the excess energy created from the alternative sources to be stored and released when needed. This would allow previously generated energy from wind turbines or solar panels to be used for present demand, minimizing fossil fuels

from being used and allowing renewable energy to be a larger contributor to electricity in the grid (QuinteQ Energy Storage, 2014).

There are currently many technologies that are being researched and developed into viable energy storage systems. One such system is the metal-air battery, e.g. zinc-air battery, which utilizes an oxidizable metal, alkaline electrolyte, and air to produce an electrochemical reaction and generate power. One major advantage of metal-air batteries over conventional batteries is that they have the highest theoretical specific energy densities on the account of oxygen in the air, an unlimited resource, being the active material at the battery cathode. A major drawback of metal-air batteries is their lack of rechargeability because of dendrite formation and carbonation of the alkaline electrolyte solution (Crompton, 1996).

Another promising candidate at filling energy storage demands is the flow battery (Weber, et al., 2011). In this technology, two liquid electrolytes are used to power the electrochemical reaction via oxidation-reduction. One of the benefits of flow batteries is the ability to be scaled up efficiently, as power and capacity are decoupled. This creates an independence between the two, where power is proportional to the size of the stack, and capacity is proportional to the amount of active material stored. These systems usually have better kinetics than conventional batteries due to operating in the liquid phase. The most prominent limitations to flow batteries are the high capital costs and relatively fledgling research compared to other energy storage technologies.

A third, viable energy storage is the liquid-metal battery (Kim, et al., 2009). In general, liquid-metal batteries consist of two different molten metals and a molten salt electrolyte that are all of varying densities. In these systems, one molten metal becomes oxidized upon discharge, where the ion travels through the electrolyte and alloys with the secondary molten metal. Upon charging, this alloy gets broken down back into the secondary metal atom and the ion, where the

ion travels the electrolyte and gets reduced back as the molten metal. The major advantages of liquid-metal batteries are their superior conductivity and kinetics since the liquid phase interactions allow for better mass transfer between the different liquid phases. On the other hand, liquid-metal batteries generally have low voltages and are operationally sensitive because the battery requires the proper separation of the three liquids. If perturbed, runaway reactions could occur, since the alloying reaction is often exothermic, leading to mechanical breakdowns and operational failure.

Due to the various problems of the current electrochemical energy storage options, liquid metal-air batteries were proposed to overcome them (Howard, et al., 2015). The benefits of liquid metal-air include properties such as high energy density, prevention of dendrite formation, and relatively long life cycles. One major hindrance of this battery type is their relatively high operating temperatures. This leads to the investigation of using low melting point metals and alloys as the active material in the anode, such gallium, indium, and tin alloys. For this research proposal, gallium was chosen based on previously conducted research by Howard, et al. (2015).

This research was focused on further investigating and improving the performance of this gallium-air battery developed by Howard, et al. (2015). Last year's project designed and tested a prototype gallium-air battery using the Swagelok cell design. A proof of concept was achieved when the battery could maintain an open circuit voltage ranging from 1.1 to 1.4 V and reproducible discharge performances. This proved the feasibility of gallium-air and that it is worth investigating further.

This report summarizes the work that was accomplished and the progress made. Chapter 2 begins with a literature review that discusses the necessity of grid-scale energy storage due to the increasing number of renewable energy sources being incorporated into the grid. The benefits and limitations of current energy storage systems being used are summarized. These systems are flow

battery, metal-air battery, and liquid metal batteries. The design of the liquid gallium-air battery was inspired by taking the advantages of the aforementioned technologies without the hindrance of commonly known limitations.

In Chapter 3, we described the methodology adopted from Howard, et al. (2015). The structural setup of the gallium-air battery was discussed. The software program used to conduct the experiments was also mentioned in detail for the discharge and charge steps. Both structural and software setup were kept consistent for all tests in order to compare performances when a particular parameter is manipulated.

The results of critical experiments are located in Chapter. Some experiments were conducted using the same test setup to validate the results from Howard, et al. (2015). This ensured that the methodology adopted was consistent. After validating their results, optimization of the system could be conducted to improve the discharge duration and performance. Once the optimal conditions were determined, regeneration of the electrolyte was investigated to determine the feasibility of a flow battery schematic, where the electrolyte would cycle continuously through the system.

In Chapter 5, conclusions were stated and recommendations were made. Important factors that affect the performance of the system were determined. Further investigation should be made to determine the feasibility of recharging the gallium-air battery and a flow battery scheme that would allow the gallium-air battery to become a grid-scale energy storage.

The Appendices provide, in greater detail, the complete guide to assemble the components of the battery, along with initiating experiments.

CHAPTER 2: LITERATURE REVIEW

2.1: Energy Storage

In today's world, energy consumption is projected to rise, as the global population continues to increase and countries are beginning to modernize and grow into industrial centers. As the world continues to urbanize and industrialize, energy consumption is rapidly growing as a necessary commodity, with upward projections of 37 percent by 2040 (Howard, et al., 2015). In the United States alone, over 85 percent of the energy that is harvested for consumption is derived from fossil fuels, with over a quarter of that energy being extracted from coal, the most carbon-intensive form of energy (Weber et al., 2011), and a mere 6.6 percent being generated from renewable sources (Ibrahim, 2008). Furthermore, as of 2008, electrical energy made up 12 percent of the world's total energy consumption, with an expected rise to 34 percent by 2025 (Ibrahim, 2008). However, with increasing energy production, the environmental consequences produced by fossil fuel consumption must be controlled and the integration of renewable energy has to occur before climate change can be addressed.

Many countries are beginning to further integrate renewable energies, such as wind, solar, and hydroelectric, into their electrical grids to minimize their dependence on carbon-intensive fuels. In the United States, over thirty states have enacted renewable portfolio standards, which are regulations by the government that require a certain percentage of the state's electricity to be from renewable resources prior to a certain year (Eastin, 2014). However, as attractive as this idea may be, increasing the amount of electrical energy derived from these renewable but intermittent sources can be harmful to the grid if the proper precautions are not implemented, as the electrical system has virtually no storage capacity and instantaneous demand and supply can be matched. Since renewable energies, especially solar and wind, are often highly intermittent, Weber, et al.

(2011) states that if renewable energies exceed twenty percent of the electrical energy generation, the grid becomes highly unstable as there would not be enough energy to supply to consumers during this intermittent periods. Frequently, these renewable resources also generate the most electricity during non-peak consumption hours, as shown in Figure 1, which poses the recurring issue of utilizing less efficient, less controlled coal-fired plants supply to the grid to help the demand of peak hours. Since an increasing number of states are enforcing renewable portfolios, this twenty percent limit is quickly being approached, which means that new technologies and innovative ideas, especially energy storage devices, must be researched and implemented to help alleviate this issue.

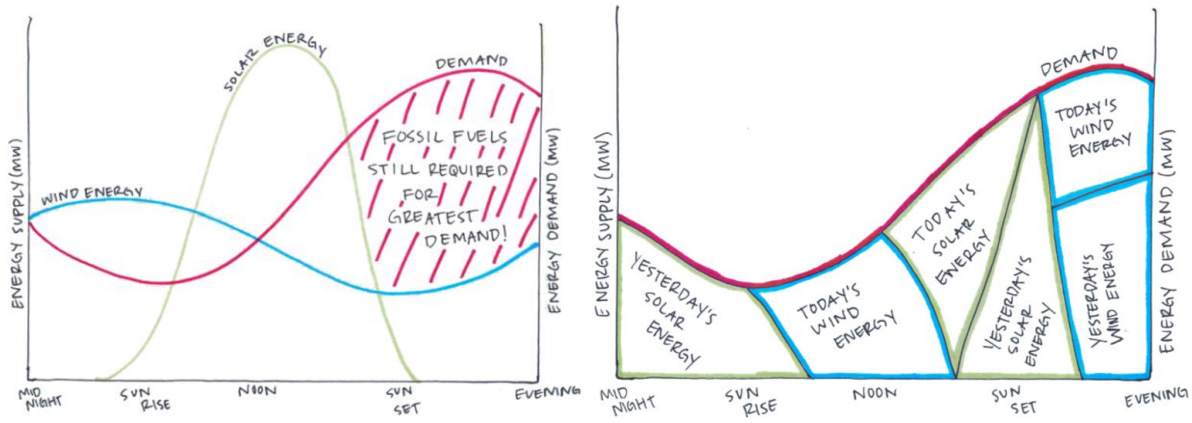

Figure 1: Qualitative plots of energy consumption and renewable energy production throughout the day (left) and the ideal situation using energy storage (right) (QuinteQ Energy Storage, 2014)

Energy storage devices and technologies are systems that take electrical energy and store it as various forms of kinetic and potential energy, such as chemical, gravitational, or thermal, as shown in Figure 2 (Ibrahim, 2008).

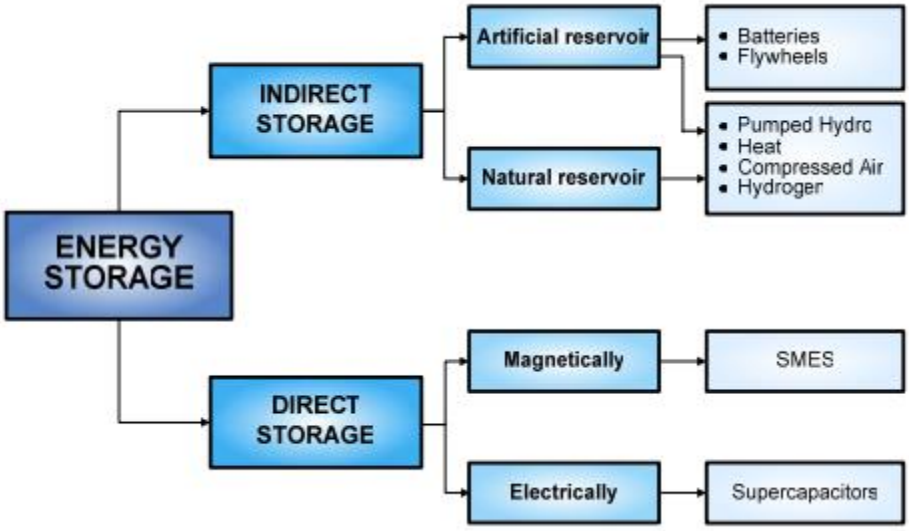

Figure 2: Storage technologies classification (San Martin, et. al, 2011)

The most common forms of energy storage include the following:

- Pumped hydro storage is a form of storage where excess electricity is used to power pumps that push water from downstream back to a higher reservoir location. When energy demands peak again, these systems allow water to flow back down to a lower elevation, spinning a turbine or generator in the process. These systems can store upwards to tens of gigawatt-hours and are very efficient. They work very well with conjunction with a hydroelectric dam but are highly site specific (Ibrahim, 2008).
- Chemical storage devices, such as lithium-ion, lead-acid, or nickel-metal hydride batteries, are often used in portable devices and load shifting in grid applications. These devices involve the electrode to act as an accumulator, where the active material that stores electrical energy as chemical energy, is deposited into the electrodes as part of the charge-discharge cycle. However, for grid level storage, a very large number of rechargeable batteries are needed, which is generally not cost effective (Ibrahim, 2008).

- Flow batteries are a specific type of batteries that have the ability to separate the system's power from the energy storage capacity, much like a fuel cell. These batteries often utilize separate aqueous electrolytes that store electrical energy in the form of chemical energy via reduction-oxidation reactions between the two electrolytes. This system has the capability of storing megawatt-hours' worth of energy. While many flow batteries are in advanced development stages, they have not so far been implemented widely. Cost and low energy density remain as hurdles (Weber, et al., 2011).

Since energy storage comes in various forms, chemistries, and mechanical structures, not every form of storage can be applied to all sectors. Each storage technology often has its own unique purpose based on their application. These purposes encompass considerations of portability, storage duration, short or long term usage, and the maximum amount of energy that can be drawn from the storage at any one moment. In general, energy storage technologies are often defined by six major parameters that dictate their definitive application and usage. These include the following:

1. **Storage capacity:** the total amount of energy that can be stored in the device
2. **Energy available:** the amount of usable energy that can be drawn out of a device, often dictated as a percentage of the total storage capacity
3. **Discharge time:** the length of time to discharge total storage capacity at peak power
4. **Efficiency:** the ratio of energy released over the total stored energy
5. **Durability:** number of cycles of charge and discharge that the system can consistently execute before becoming unusable

6. **Autonomy:** length of time that the device can continuously draw maximum power until all usable energy is consumed

In order to utilize the energy generated by renewable sources such as wind turbines or solar panels that would otherwise be lost when not consumed, a considerable amount of research has focused on energy storage that could handle the large energy capacity from the grid. In the current situation, roughly 2.5 percent of the electricity transferred to the United States of America originated from pumped hydroelectric storage. However, this percentage is low when compared to those of Europe and Japan, which are 10 and 15 percent, respectively. There are four different types of large-scale energy storage: mechanical, electrical, chemical, and electrochemical. The pumped hydroelectric storage is responsible for the majority of the global storage capacity (127,000 MW) while compressed air storage follows with 440 MW (Dunn, et al., 2011). Since the 1920s, pumped hydroelectric has been used to balance the fluctuations of load in the grid system. It is often used for energy storage since it can respond in seconds when there is a large deviation in the load of the system. Another advantage is its flexibility to increase in capacity in order to accommodate the fluctuation, either by manipulating the size or the amount of units (Energy Storage Association, n.d.). Variation in size is not an issue because the system is composed of cheap materials (such as concrete, water, and dirt) that can last for an extended period of 40 years. With simple materials, the plant is low maintenance, with a round-trip efficiency of roughly 65 to 75 percent. The disadvantage of pumped hydroelectric plant is its limitation to geography since not all places have the space elevation, or adequate amount of water (Dunn, et al., 2011).

In order to compete with the pumped hydroelectric storage, other energy storage devices must have the ability to respond quickly to a large load at peak time and load shifting. Load shifting is when the technology would store excess energy in the system and release energy when

demanded. There are four types of energy storage: mechanical, electrical, chemical, and electrochemical. As shown in Figure 3, a variety of energy storage technologies are being compared in two aspects, discharge time period and power ratings, which is the amount of power required. Some of the technology involved are supercapacitors, batteries, flywheels, pumped hydroelectric, and compressed air energy storage (Dunn, et al., 2011).

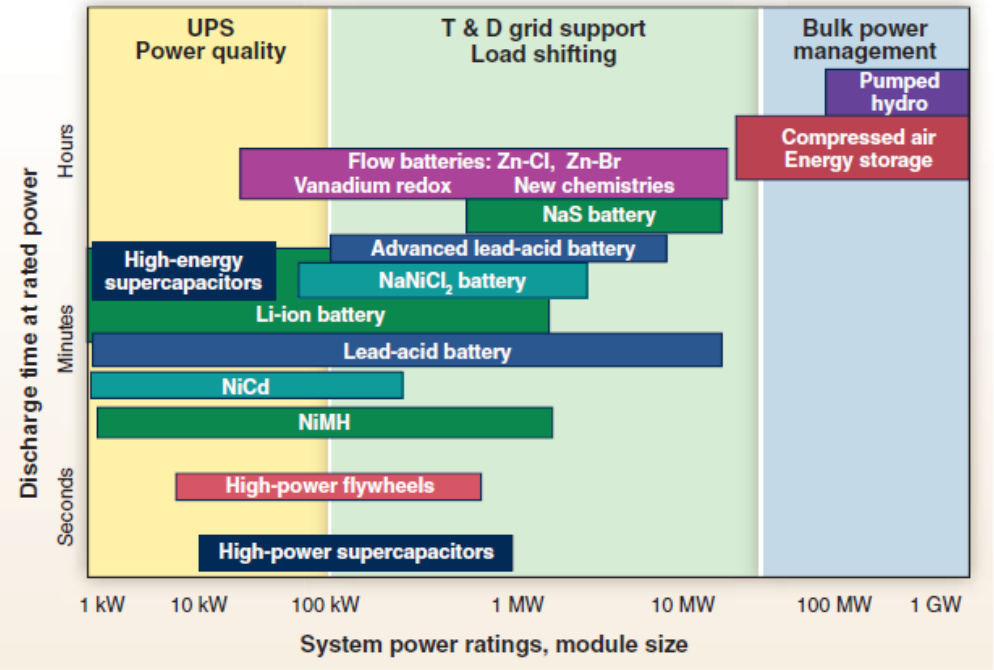

Figure 3: Comparison among different types of energy storage in terms of discharge period and power ratings (Dunn, et al., 2011)

As renewable portfolios are paving the pathway for heightened integration of sustainable, non-carbon emitting technologies, energy storage must also be further developed. Currently, the grid experiences large fluctuations of energy demand and generation, based off the time of day and season, as shown in Figure 4 (Huggins, 2010).

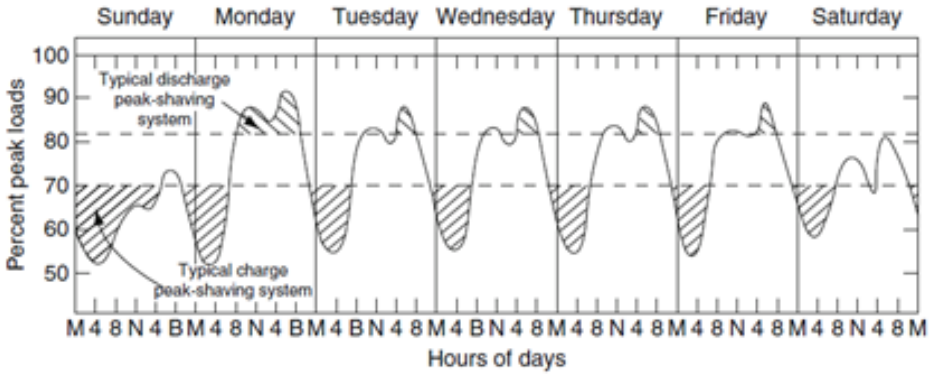

Figure.4: Hourly data on electric load during a full week, showing possible use of an energy storage system (Huggins, 2010)

Instead of using those poor efficiency, coal-fired power plants, these disturbances could be mitigated by two main ways: load shifting and energy storage. In load shifting, the electrical grid must be updated to a SmartGRID, where appliances and applications that are not time-specific are ran and completed in times where there is minimized power demand. The major disadvantage with this mitigation method is that much of the grid would have to be renovated and consumers would need to update their devices and appliances to fit this new infrastructure. On the other hand, energy storage would help mitigate these peak-level demands by absorbing excess electrical energy from renewable energies, or absorbing electrical energy at the cheapest costs, and supplying it back to the grid. This concept is shown in Figure 5, where the curves represent the power demand that must be generated instantaneously, often from those carbon-intensive fuels. The flat line in this figure represents the ideal conditions of the power that must be generated instantaneously if energy storage is implemented, effectively eliminating peaks and troughs.

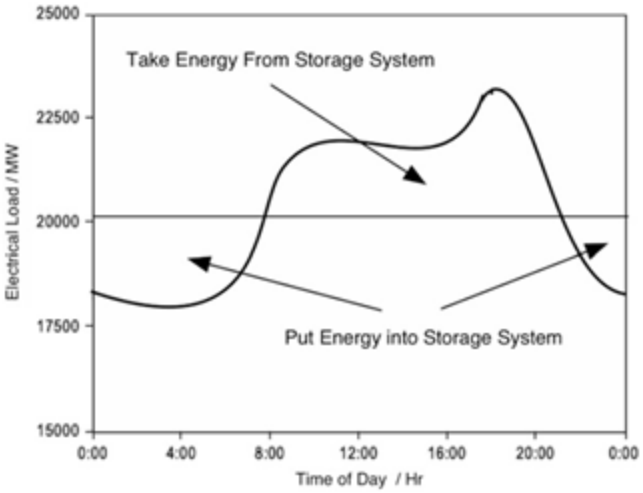

Figure 5: Ideal situation in which energy storage methods flatten the time-dependence of the energy-supply requirement (Huggins, 2010)

2.2: Chemistry of Batteries

Batteries have been integrated into a majority of devices that are used on a daily basis to provide portable energy storage. They are responsible for transforming chemical energy to electrical energy through electrochemical oxidation-reduction (redox) reactions in order for devices to function. Redox reactions occur when there are exchanges of electrons between two materials, causing the loss and gain of electrons. In order to carry out redox reactions, batteries consist of three main components: an anode, a cathode, and an electrolyte. Metals, like zinc and lithium, are often utilized as the anode material and oxidizes since they easily give up electrons, have high conductivity, stability, and low cost. However, other materials have also been adopted for advanced batteries (Linden, 1984). The cathode is the material that accepts electrons from the anode, which are then reduced in the cathode reaction. The majority of cathodes are composed of metal oxides since they are good oxidizing agents. The electrolyte acts as the ionic conductor for charge transfer and charge balancing between the cathode and anode. This movement of the electrons is the key to powering electronic devices. The electrolyte is typically a solution composed

of salts, acids, or bases in some solvent. However, the electrolyte must be non-reactive with the anode and cathode, safe for usage, and independent of temperature variations (Linden, 1984).

Together, the three main components make up what is known as the electrochemical cell. Some batteries can compose of multiple cells to form a stack to provide a higher voltage or current. To prevent the cell from short-circuiting, the separator is responsible for partitioning the anode and cathode components. However, instead of an impenetrable barrier, the separator must be permeable for the electrolyte to have ionic conductivity necessary to transfer these charges. Although research has been conducted for more than an era, many studies are still focused on improving the battery technology to make it more efficient. The ideal characteristics for batteries include a high energy capacity and cell voltage while still being inexpensive, light, and safe for use (Linden, 1984).

Batteries are divided into primary and secondary battery depending on their rechargeability. Primary batteries only have a singular discharge cycle. Despite its inability to recharge, it has the advantage of low cost, high energy density, and long shelf life. Some examples of commonly used primary batteries are alkaline and lithium-oxide batteries. Secondary batteries can be discharged and charged multiple times, making it ideal for energy storage. However, the energy density and charge retention are lower than the performance of primary batteries in addition to being more costly (Linden, 1984). Nickel-metal hydride, lead-acid, and Li-ion batteries are rechargeable batteries available for consumers.

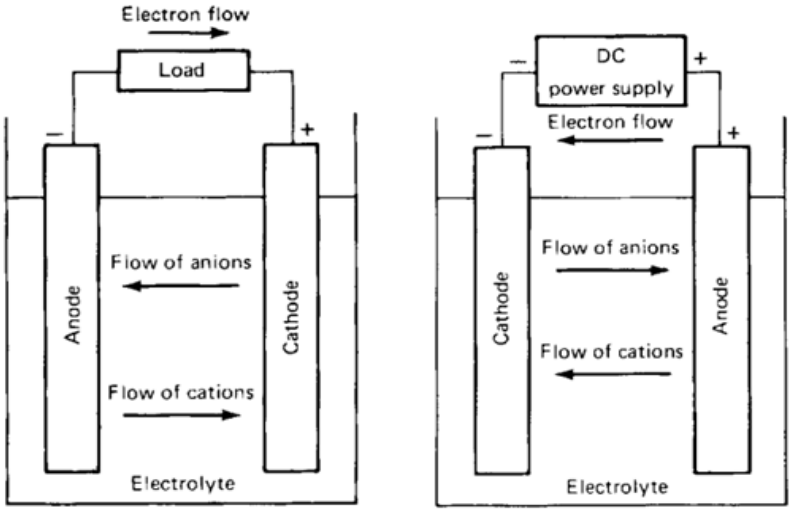

Figure 6: Schematic of a generic battery, showing the flow of electrons and ions from the two electrodes. When discharging (left), the electrons go from anode to cathode while the anions flow to anode and cations flow to cathode. The reverse occurs for charging (right), when electrons go from cathode to anode while the anions flow to anode and cations flow to the cathode (Linden, 1984)

There are two modes of operation that a secondary battery can be in: discharge and charge. Discharge occurs when there is a flow of electrons from the anode to cathode through a load. A load is any device that requires a flow of electrons to operate. To have a closed circuit, the anions flow to the anode or the cations flow to the cathode within the electrolyte. Charge mode is the reverse of discharge mode; wherein a power source provides the energy to reverse the flow of electrons from the cathode and go to the anode side instead (Linden, 1984). A schematic of the two operations can be seen in Figure 6.

2.3 Batteries on Grid Scale

There are more batteries presented in Figure 7 than other form of energy storage since their compact size allows them to be implemented anywhere. Batteries also have flexible power and energy properties with long cycle life and do not require much maintenance. One of the main factors that prevent batteries from being widespread is their high cost and bulk. However, as more

research is being done to enhance their efficiency and scalability, their costs are continuing to drop, making batteries more accessible to be implemented. Figure 7 compares many types of rechargeable batteries in terms of specific power and specific energy. Based on the comparison, lithium-ion batteries appear to perform at least 2.5 times better than other types of battery, in terms of possessing both high specific power and specific energy. (Dunn, et al., 2011).

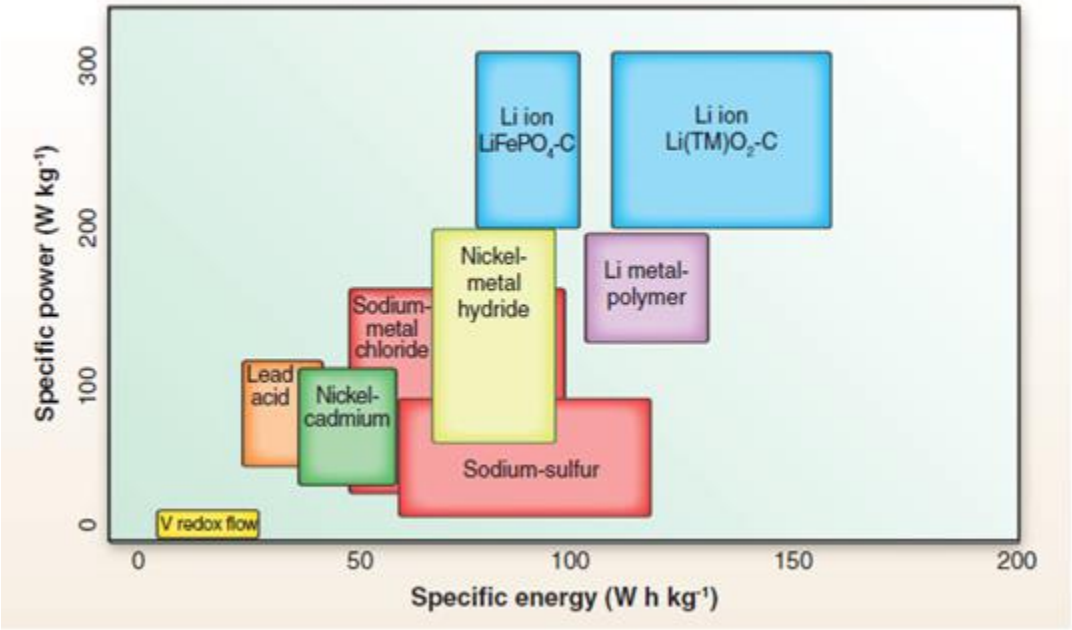

Figure 7: Comparison of rechargeable batteries based on specific power and specific energy (Dunn, et al., 2011)

Lithium-ion batteries operate by transferring Li ions across the electrolyte from the anode (composed of graphene structure holding the Li ions) to the cathode ($LiMO_2$ layer structure) when discharging as shown in Figure 8. The battery has many advantages that makes it attractive for grid-scale storage. These include high cell voltage, high energy densities, low molecular weights, long life cycles, and rate capabilities. However, research and development is still being conducted to increase safety and performance aspects while lowering the price (Dunn, et al., 2011). Li-ion batteries can have safety concerns as the organic solvents used for solvating the electrolyte in the

separator could cause the cell to expand or ignite if mismanaged. (Young, et al., 2013). Even so, they are well integrated in many electronics and hybrid electric vehicles with the potential for implementation in grid applications in the future. Other studies are also developing Li-O_2 (a primary battery) and Li-air batteries in order to make them competitive and applicable for grid and automotive applications. Once lithium batteries could be implemented in those applications, the demand for lithium might jeopardize the world resources. Due to this concern, sodium could be a substitute since it is plentiful, cheap, and its intercalation chemistry is similar to lithium. However, sodium has a higher molecular weight and lower energy density in comparison (Dunn, et al., 2011).

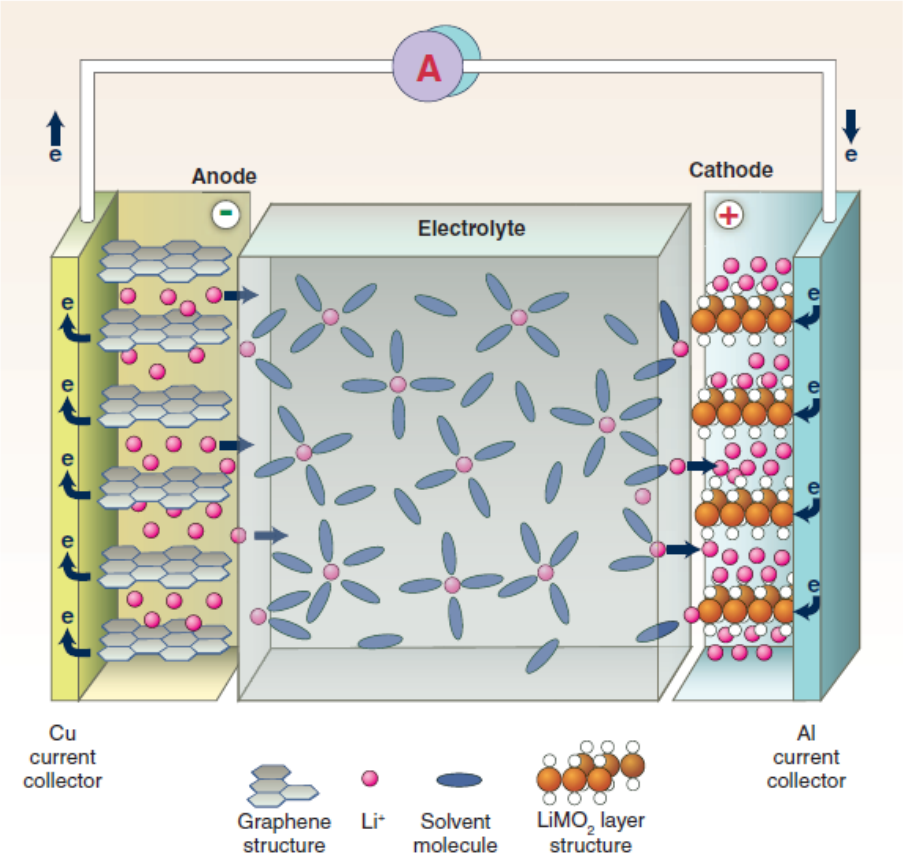

Figure 8 Schematic of Li-ion battery (Dunn, et al., 2011)

The sodium/sulfur (Na/S) battery has in fact been used for energy storage on the grid globally, contributing about 315 MW of discharge power. It was adopted by Japan in 2002 for

"utility-based load-leveling and peak shaving applications" since it has small footprints, cycling flexibility, and little maintenance costs (Dunn, et al., 2011). The battery operates at high temperature, ranging from 270^{o}C to 350^{o}C, for adequate conductivity of solid-phase beta-alumina used as the Na ion membrane. The elevated temperature is also necessary to maintain the electrodes (sodium and sulfur) in the molten state, allowing Na ions to transfer across the conducting membrane, shown in Figure 9. Interestingly, the beta-alumina ceramic tube is the main element that affects the performance and price of the battery. Current research focuses on scaling the membrane with suitable mechanical and electrical characteristics since any fracture could lead to battery failure. Problems that are encountered relate to thermal control, costs, and proper sealing. Since the battery operates at high temperatures and has highly reactive molten electrodes, the seals are vital for the cell to function properly and safely, not allowing components to interact. In terms of thermal controls, the temperature of the cell does fluctuate depending on the mode of operation. The temperature increases when discharging, but decreases when charging. Therefore, the materials in the cell must be able to withstand a wide range of temperatures in addition to corrosion. Both sulfur and polysulfides are corrosive so finding an inexpensive container is no simple task. For low-cost alternatives, carbides could be used as a resistant coating against the corrosion due to sulfur (Dunn, et al., 2011).

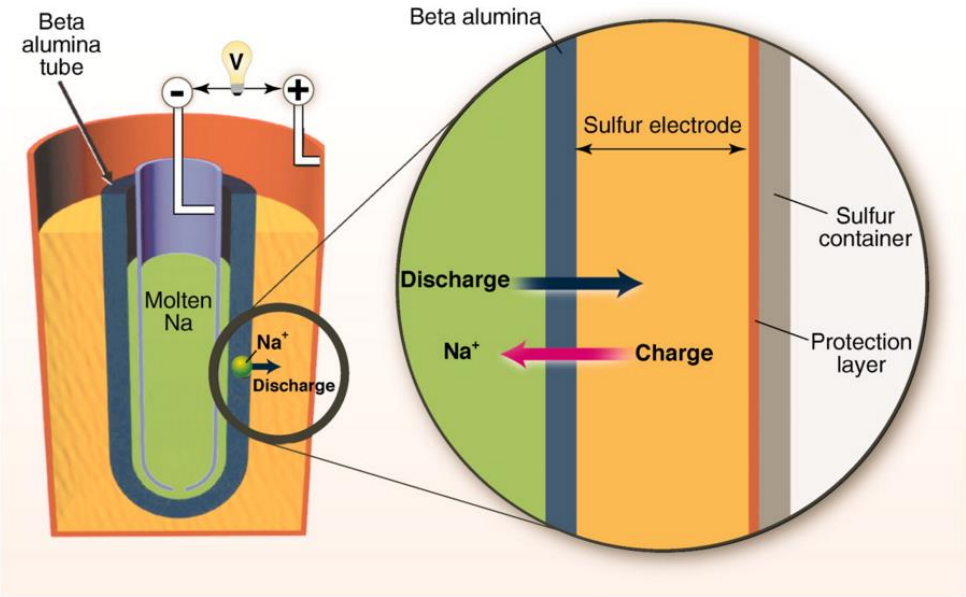

Figure 9: Schematic of the components of Na/S battery. The molten Na in the middle (green) is the negative electrode and the molten S (yellow) is the positive electrode. The beta-alumina tube acts as the conducting membrane between the two electrodes. In discharge, the Na ion goes from the molten Na to sulfur and the reverse is true for charging (Dunn et al., 2011)

2.4: Metal-Air Batteries

Metal-air batteries were discovered in 1868 by Leclanche using a MnO_2/carbon cathode and have developed since then to be practical to use (Neburchilov, et al., 2010). The battery consists of using a metal for the anode and air as the cathode with an alkaline electrolyte in between the two electrodes. Due to the unlimited source of air as the cathode, the metal-air battery has one of the highest energy capacities. Since air is available from the surrounding, it does not occupy any space of the cell (Zhang, et al., 2015). As shown in Figure 10, the metal is oxidized, releasing electrons to the system. Simultaneously, the air enters through the cathode through constructed openings to allow it to enter the system. The air accepts the electrons produced and subsequently gets reduced to oxygen-containing species. The metal ions and oxygen-containing species travel across the electrolyte and form metal oxides in the process (Cheng & Chen, 2011). This cycle continues to generate a stream of electrons to power devices.

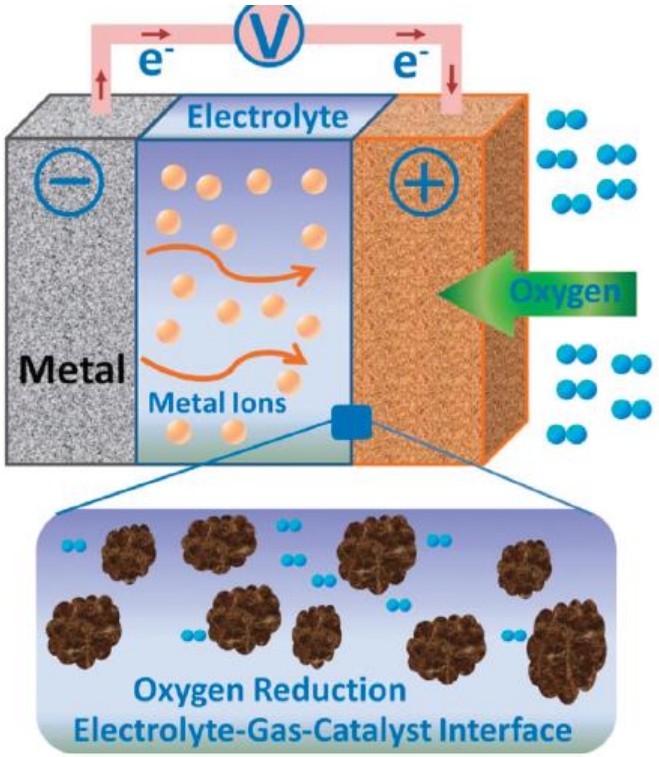

Figure 10: Schematic of the chemistry of metal-air battery (Cheng & Chen, 2011)

The electrochemical reactions and products of metal-air batteries vary depending on the metal anode, electrolyte, and catalyst used in the gas diffusion layer. Table 1 summarizes the common metal-air batteries with their reactions and theoretical standard potentials (Cheng & Chen, 2011).

Table 1: Summary of metal-air battery reactions and standard potential (Cheng & Chen, 2011)

Metal air cells	Anode (a) and overall (o) reactions	E^0/V[a]
Zn–air	(a) $Zn + 2OH^- \rightarrow ZnO + H_2O + 2e$	−1.25
	(o) $2Zn + O_2 \rightarrow 2ZnO$	1.65
Mg–air	(a) $2Mg + 4OH^- \rightarrow 2Mg(OH)_2 + 4e$	−2.69
	(o) $2Mg + O_2 + 2H_2O \rightarrow 2Mg(OH)_2$	3.09
Al–air	(a) $Al + 3OH^- \rightarrow Al(OH)_3 + 3e$	−2.31
	(o) $4Al + 3O_2 + 6H_2O \rightarrow Al(OH)_3$	2.71
Li–air	(a) $Li + OH^- \rightarrow LiOH + e$	−2.95
	(o) $4Li + O_2 + 2H_2O \rightarrow 4LiOH$	3.35

[a] The standard potentials (E^0) are given by assuming a potential of 0.40 V for the cathode reaction. All potentials are reported *vs.* the standard hydrogen electrode (SHE).

Compared to other primary batteries, zinc-air can provide high currents over a long period of time without much fluctuation in voltage (Crompton, 1996). Due to its low cost and environmentally safe nature, zinc-air batteries are the most common metal-air battery being commercialized for electronics and have the potential to be utilized for electric vehicles and grid applications (Zhang, et al., 2015). The reactions for both the anode and the cathode of the zinc-air cell are shown in Table 4 (Howard, et al., 2015). Al-air and Mg-air are also used for military applications. Since zinc, aluminum, and magnesium are abundant earth-elements, development and utilization of metal-air can still expand in terms of commercial applications and large-scale production (Cheng & Chen, 2011).

Due to their high energy densities, zinc-air button cells are often used for hearing aid applications, shown in Figure 11. At the early stages of development, it encountered issues with allowing air into the cell without having electrolyte leakage. In addition, when discharging the battery for extended periods, carbonation of electrolyte would occur. The zinc-air components are made of a PTFE-laminated charcoal catalyzer with manganese oxide as the catalyst for the cathode, zinc with slurry of electrolyte (potassium hydroxide) for high energy density on the anode, and the porous separators used are multilayers that still allow ions to travel through. The layers allow long period for discharge for low currents. The volumetric specific energy density of the zinc-air is roughly 650-800 mWh/cm^3, which is high when compared to its competitors that have under 520 mWh/cm^3 (mercury-zinc, silver-zinc, alkaline manganese dioxide cells). The battery can operate in a range of temperature, from -10^oC to 60^oC, with an open circuit voltage (OCV) of 1.15 to 1.3 V. In order to ensure long shelf life, the air holes on the cathode side are shielded by a thin foil layer to prevent the air from activating the battery. This is removed when pressed into service. The

electrolyte moisture content is also managed by using a hydrophobic gas diffusion layer (PTFE) at the cathode (Crompton, 1996).

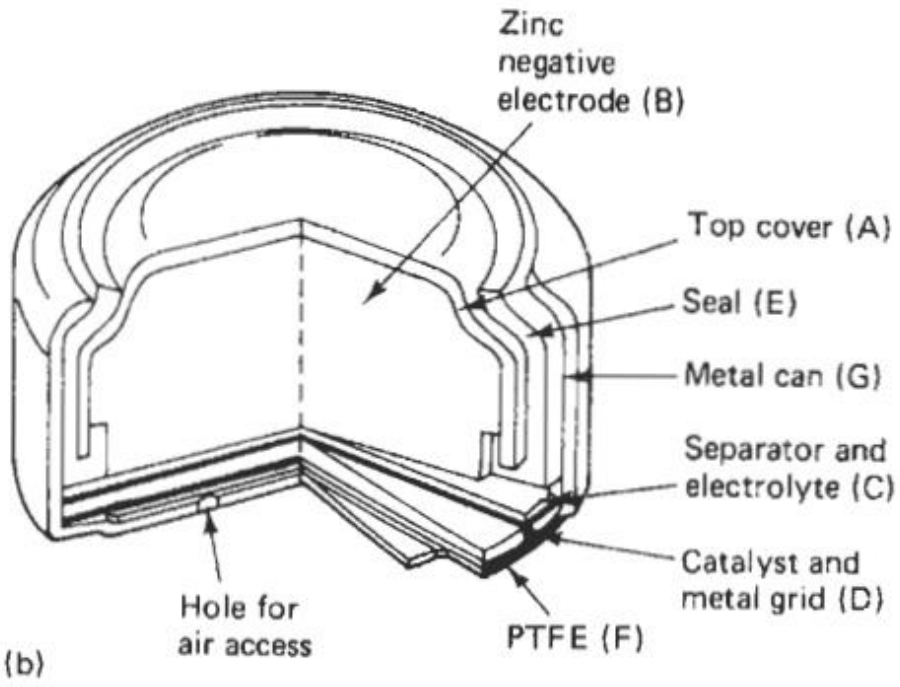

Figure 11: Diagram of the components within a zinc-air button cell (Crompton, 1996)

While the metal-air battery has a number of positive factors that make it favorable for energy storage, it is hindered by rechargeability. It can be recharged if the components in the battery are replaceable by inputting new metal and electrolyte into the system. There have been recommendations on having the metal anode and electrolyte continuously cycled, rather than immobilized, in order to make rechargeability possible (Cheng & Chen, 2011). Many research has been established to develop the rechargeable zinc-air battery with promising results. Unfortunately, zinc dendrite growth through the separator can occur, which leads to short-circuiting after some cycles. For this issue, finding a different separator that could prevent this phenomenon would solve the problem. In terms of the catalyst on the air electrode, platinum has been used for the oxygen-evolution reaction for discharging mode but it does not perform well

when charging since it “acts as a low hydrogen overvoltage site”. In this case, unless materials could accommodate for that inability, a third electrode would be needed for charging mode (Crompton, 1996).

A metal-air battery system has to deal with low efficiencies since it does not fully take advantage of the anode. There is a passivation and corrosion of the anode side that transfer to the electrolytes. The circulation of metal oxides and hydroxides delay the interaction with electrolyte. This results in the shortage of discharge and the untouched materials on the anode side (Cheng & Chen, 2011). Zinc-air batteries are also limited by the catalyst used in the cathode. Traditionally, platinum is used for the oxygen-evolution reaction during recharging, and metal oxide, such as MnO_2, is for oxygen-reduction reaction during discharging. These catalysts have high costs with disadvantages in selectivity and stability. To tackle this problem, research and development teams have been proposing metal-free catalysts by using mesoporous nanocarbon foam doped with nitrogen and phosphorus for both oxygen evolution and reduction that would have equivalent or higher performance than the current catalysts used in zinc-air. The results were promising and comparable to the commercial zinc-air (with the current density of 60 mA/cm^2 versus 70 mA/cm^2 respectively) but further optimization is necessary before the catalyst could be implemented (Zhang, et al., 2015).

2.5: Flow Batteries

As part of the new developments in the energy storage industry, redox flow batteries are beginning to garner attention as they are becoming more viable for grid-wide energy storage. Flow batteries usually consist of a cell stack, with tanks to store aqueous electrolytes that exhibit reduction-oxidation reactions to store and deliver energy, as shown in Figure 12.

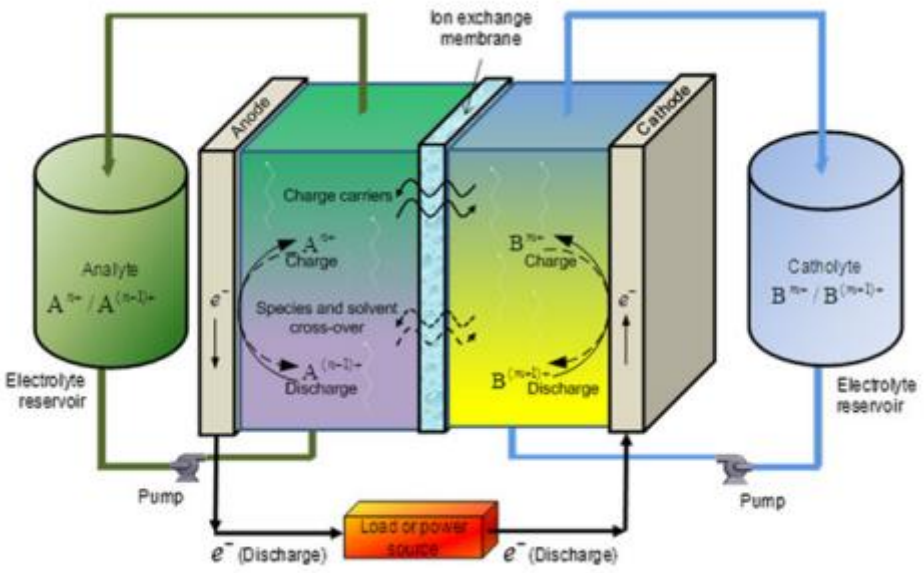

Figure 12: Schematic diagram of a redox flow battery (Weber, et al., 2011)

In a redox flow battery, the overall stack consists of multiple cells built together using bipolar plates to ensure electrical connectivity from one unit cell to the next; that current flows in series, resulting in a summation effect for voltage (Wang, 2010; Weber, et al., 2011). In each unit cell, the anode and the cathode are separated by an ionic exchange membrane, which helps to keep the two electrolytes from mixing. These membranes are also important for moving charge carriers on charge and discharge cycles so that the system each side of the cell is balanced in terms of charges if the chemistry requires it. On both the anode and the cathode, there are porous electrodes, often graphitic, which help to generate and transport electrons from the stack to the external circuit. In general, a redox flow battery upon discharge, has an anolyte (or a more negative electrolyte) that gets oxidized and loses an electron, goes through an external circuit, and reduces the catholyte. Upon charge, the opposite occurs where the anolyte instead gets reduced. This consistent cycle of shuffling electrons allows for redox flow batteries to often have a higher durability than other forms of batteries, as this closed system does not exhibit dendrite formation (Weber, et al., 2011).

For grid-scale energy storage, there are many advantages to using redox flow batteries. The main advantage for this technology is its unique capability of separating stack power and energy storage capacity, meaning that each can be independently scaled up. This is because the full stack is assembled using just the electrodes, bipolar plates, and ionic exchange membranes and the power output is dictated by surface area and the number of unit cells in that stack. On the other hand, the energy storage capacity is only dictated by the amount of active electrolyte material there is. By increasing the volume of electrolytes or increasing the concentrations of the active material, energy capacity can be scaled up as the amount of energy is stored in individual chemical bonds. In addition, redox flow batteries also have the physical chemistry advantage in the sense that there is no intercalation into or interaction with the electrode layer. Since the active materials are usually aqueous by nature, this interface layer strictly acts as a transport method for electrons. This helps to reduce the need for advanced electrode designs because it will not be physically manipulated with the impregnation of active material. In theory, this also improves the durability of the electrode layer because there is no dendrite formation or shape change in the electrode over time (Weber, et al., 2011).

On the other hand, the limitations behind redox flow batteries must also be considered. The main barrier to the successful integration of flow batteries is their cost, as current redox flow batteries have estimates of $2,500 per kilowatt for capital costs, which is $1,000 more expensive than target costs. In addition, one other major limitation to redox flow batteries is the lack of available data since redox flow batteries are a relatively new technology that has just gained popularity in the recent decades. As more research is being conducted, technological limitations are being exposed, but many of these are specific to certain chemistries, but one major problem that many of these systems face is the crossover of active material through the membrane. This

membrane is meant to act as an ionic conductor for charge balancing and is used to keep the anolyte and catholyte separate. In the event that this component fails, the flow battery begins to lose capacity as active materials begin to mix (Weber, et al., 2011). There is also cross-over by passive diffusion across the ion exchange membrane.

To tackle this issue, the most popular redox flow battery in this sector is the vanadium redox flow battery, which uses vanadium sulfate for both the anolyte and catholyte. In this chemistry, the anode utilizes a V^{2+}/V^{3+} ion charge system while the cathode utilizes a V^{4+}/V^{5+} system, both of which are coupled with sulfate ions. This system is favorable in comparison to other chemistries because in the event of crossover, there are no dangerous side reactions or major loss in active materials since the vanadium ions will get reduced or oxidized to match the charge of the surrounding electrolytes. However, vanadium redox flow batteries (VRBs) are not ready for commercialization as they face many technological problems, including low solubilities and precipitation at low temperatures and degradation of the vanadium-sulfate bonds at high temperatures. Much research is currently being conducted on how to address some of these issues, including changing the supporting ligands that balance the charges on the vanadium ion (Schwenzer, et al., 2011).

2.6: Liquid Metal Batteries

Starting with initial research proposals dating back to the Cold War era, liquid metal batteries have now regained research interest as they are becoming a viable candidate for long-term energy storage. Liquid metal batteries are rechargeable cells that are composed of three different components, as shown in Figure 13.

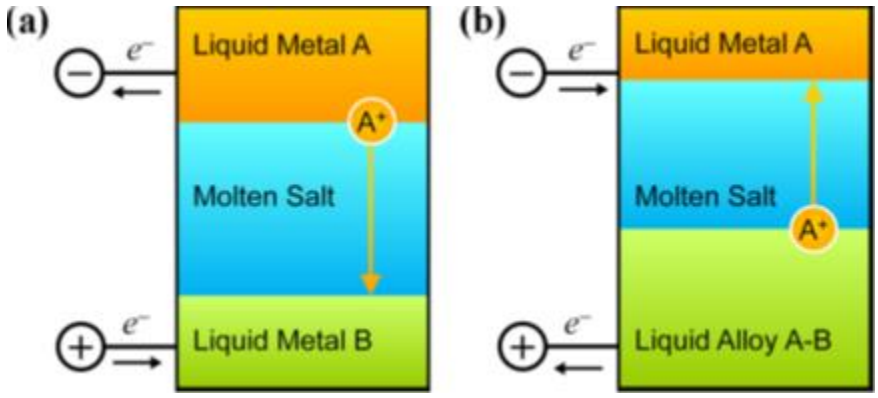

Figure 13: Schematic diagram of a liquid metal battery upon (a) discharging and (b) charging

In this type of a battery, there are two electrode layers, which consist of two different liquid metals, separated by another molten salt electrolyte layer. In order for these three phases to function properly in a liquid metal battery, their densities must be significantly different so that they naturally separate out (Kim, et al., 2009). Upon discharging a liquid metal battery, the anodic liquid metal gets oxidized, releasing the electron into the load and the metal ion into the ionically conductive molten salt electrolyte. The ion then travels through the molten salt and is reduced to metallic form and forms alloys with the cathodic liquid metal. In the reverse, charging the cell causes the alloy to separate, releasing the original metal ion to flow back through the molten salt electrolyte and get reduced to form the liquid metal atom again (Wang, et al., 2014).

To get liquid metal batteries to become viable choices of energy storage devices, three main criteria must be met. First, all the electrolytic components of the battery must be in the liquid phase within a reasonable temperature range, usually ranging 25 to 1,000^{o}C, since temperatures below 25^{o}C would require special refrigeration units and temperatures above 1,000^{o}C are hard to uniformly maintain. Second, the liquid components must exhibit superior conductivity, which is usually inherent to molten electrolytes. Lastly, for safety concerns, the active materials are required to be naturally occurring, stable isotopes so that there are no risks of nuclear radiation (Kim, et al., 2009).

Liquid metal batteries are becoming popular in the research realm as a result of their many advantages in their design and the electrochemical phenomena that occur among the liquid phases. First, liquid metal batteries are noteworthy, as they often exhibit fast kinetic rates, as the liquid-liquid electrode-electrolyte layers allow for rapid mass transfer between the several different phases. Secondly, as a result of the high temperatures and the liquid-phase electrolytes, ohmic resistances and losses are also minimized in comparison to solid electrolyte layers (Kim, et al., 2009). In addition, since all the reactions are occurring within liquid phase electrolytes in the absence of a solid electrolyte, there are no physical degradation issues, commonly seen in systems like lithium-ion batteries. As a result, this leads to increased lifetime durability as those common physical alterations and film formations often can damage other components in the cell, causing it to have a mechanical breakdown or short-circuit failure (Wang, et al., 2014).

On the other hand, liquid metal batteries also have their disadvantages. Since the existence of the three separate liquid layers are critical to the operation of the battery, this limits this technology's use to just stationary systems, as they are sensitive to any motion. In the case that they are perturbed, this runs the risks of short-circuiting the cell and promoting excess heat generation if the alloying of the two electrolytes is exothermic. Furthermore, since metals and their liquid counterparts have relatively high densities, their specific energy density is often lower than other competing technologies. In addition, most chemistries also have low equilibrium cell voltages of less than 1.0 volts, can be chemically corrosive, and high self-discharge rates in the cases where the liquid metals have a high solubility in the molten salt electrolyte. Despite these disadvantages, there is a plethora of innovative research being conducted that is looking to overcome these challenges, as these systems have much potential for grid-scale energy storage (Kim, et al., 2009).

Currently, research on these batteries looks promising and there are many corporate interests that are almost ready to commercialize their products. One example is Ambri's initial design of a three layer liquid-metal battery consisting of magnesium and antimony as their negative and positive electrodes, respectively (Lamonica, 2013). This product now has been scaled up to a 500 kW system that has the capacity to store one megawatt-hour worth of energy at competitive prices. Furthermore, this technology shows even more promise as they have transitioned to cheaper active materials and generate an even higher cell voltage. Ambri's system observes negligible degradation, shown in Figure 14, which is typical of these systems as long as they are built correctly. The result demonstrates the system to have a significant potential impact on effectively being implemented into an electric grid (Ambri, 2016).

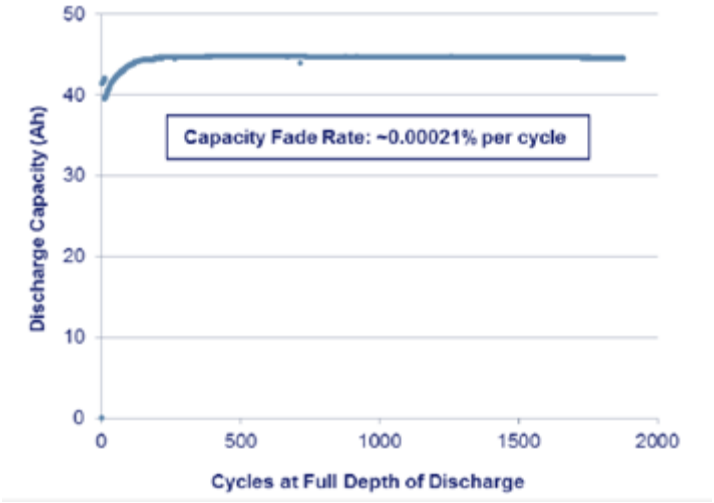

Figure 14: Discharge capacity as a function of full-depth discharge cycles of Ambri's liquid-metal system. (Ambri, 2016)

2.7: Liquid Metal-Air Batteries

Recently, liquid metal-air batteries have been proposed to solve problems plaguing metal-air, liquid metal, and flow batteries. These problems include dendrite formation, low energy density, and short life cycles. Dendrite formation is avoided due to the metal being fluid. Since the

reaction with liquid metal forms a metal oxide, the battery, theoretically, has a potential for high energy density. The properties of liquid metals also allow for the likelihood of multiple charge and discharge cycles before failing and destroying the battery (Otaegui, et al., 2014). Unfortunately, liquid metals also have their limitations. One such limiting factor is the need for the system to be maintained under high temperatures. This reduces the options for reliable energy storage. However, our choice of gallium as the liquid metal obviates this concern because of the low melting point of the gallium (Howard, et al., 2015).

2.7.1: Liquid Gallium Anode

Based primarily on literature and its attractive physical properties, despite minimal research being conducted, gallium is a prime candidate for use in a liquid metal-air battery. Gallium has a low melting point of 29.77^{o}C, minor safety concerns like skin and eye contact irritation, and minimal to no corrosion issues at low temperatures (Howard, et al., 2015). Due to a low activation energy barrier, it willingly forms oxides when exposed to an alkaline aqueous solution. The formation of oxide may create a film that would influence better transport chemistry, electrochemistry, and can cause the formation of different ions, such as $Ga(OH)_4^-$ (Chung, 2013).

Since gallium has just recently been proposed and investigated for energy storage, information on its effectiveness does not exist. Albeit this point, gallium has been used prominently in other fields. Gallium and its alloys are part of a group of metals that exhibit good semiconducting properties and are used in semiconductors and other microelectronics (Howard, et al., 2015).

2.7.2: Electrochemical Reactions

Upon discharge of the liquid gallium-air cell, as shown in Figure 15, gallium in the anode gets oxidized where it forms gallium cations and the electrons are carried through a load and then released into the cathode to reduce diatomic oxygen in air. Once this action is complete, the diatomic oxygen is reduced to negatively-charged hydroxide ions and oxygen ions, which are then transferred into the ionically conductive potassium hydroxide mixture. When these hydroxide ions reach the anode again, they form bonds with the gallium ions to form gallium oxide and/or gallium hydroxides (Howard, et al., 2015).

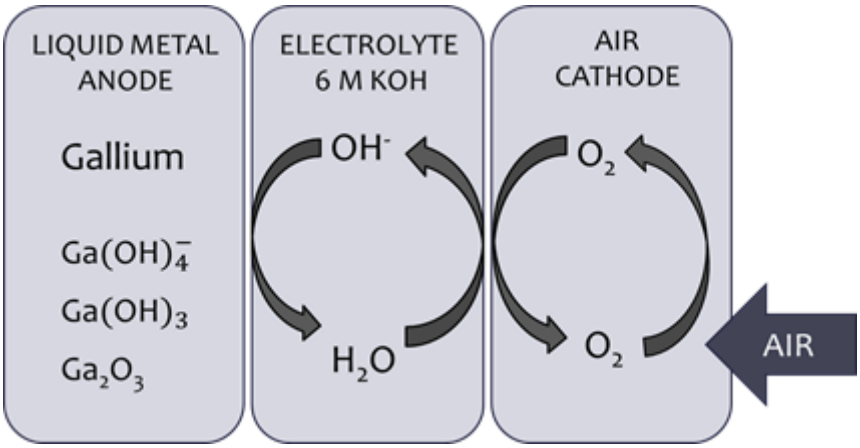

Figure 15: Diagram of the electrochemical reactions of the gallium-air cell

Using thermodynamic and electrochemical relationships and theory, it can be seen that the motivation behind using the gallium-air electrochemical cell has its merits. Using the standard Gibbs free energy and Nernst equations, as shown in Equations 1 and 2, the open circuit potential voltages and its respective free energy values for each reaction of the gallium-air electrodes in the case where gallium-oxide is formed are shown in Table 2 whereas the situation where gallium-hydroxide is formed are shown in Table 3 (Howard, et al., 2015).

$$\Delta G^0 = -nFV^0_{rxn} \quad (1)$$

$$E = E^0 = \frac{RT}{nF} \ln \frac{[Ox]}{[Red]} \quad (2)$$

From the data that is shown, it is clear that the two different reactions have different open circuit voltages, but it is still unknown which reaction dominates the electrochemical pathway. However, even the formation of gallium oxide, which has the lower of the two values for the theoretical open circuit voltage, is still very much comparable to the theoretical value found for commercial zinc-air batteries, as shown in Table 4 (Howard, et al., 2015).

Table 2: Open Circuit Voltage Calculations for the Formation of a Ga-Air Battery Assuming Gallium Hydroxide is formed (Howard, et al., 2015)

Electrode	Reaction	Potential (V)	ΔG^0 (kJ/mol)
Anode	$Ga + 4OH^- \rightleftharpoons Ga(OH)_4^- + 3e^-$		
Anode	$Ga(OH)_4^- \rightleftharpoons Ga(OH)_3 + OH^-$		
Overall Anode	$Ga + 3OH^- \rightleftharpoons Ga(OH)_3 + 3e^-$	$V_A^0 = -1.242$	-360
Cathode	$O_2 + 2H_2O + 4e^- \rightleftharpoons 4OH^-$	$V_C^0 = +0.401$	-155
Overall	$Ga + \frac{3}{4}O_2 + \frac{3}{2}H_2O \rightleftharpoons Ga(OH)_3$	$V^0 = V_c^0 - V_a^0$ $V^0 = 1.643\ V$	-476

Table 3: Open Circuit Voltage Calculation for the Formation of a Ga-Air Battery Assuming Gallium Oxide is Formed (Howard, et al., 2015)

Electrode	Reaction	Potential	$\Delta G^0\ (kJ/mol)$
Anode	$Ga + 4OH^- \rightleftharpoons Ga(OH)_4^- + 3e^-$		
Anode	$Ga(OH)_4^- \rightleftharpoons Ga(OH)_3 + OH^-$		
Anode	$Ga(OH)_3 \rightleftharpoons Ga_2O_3 + 3H_2O$		
Overall Anode	$Ga + 3OH^- \rightleftharpoons \frac{1}{2}Ga_2O_3 + \frac{3}{2}H_2O + 3e^-$	$V_A^0 = -1.323$	-383
Cathode	$O_2 + 2H_2O + 4e^- \rightleftharpoons 4OH^-$	$V_C^0 = +0.401$	-155
Overall	$Ga + \frac{3}{4}O_2 \rightleftharpoons \frac{1}{2}Ga_2O_3$	$V^0 = V_c^0 - V_a^0$ $V^0 = 1.724\ V$	-499

Table 4: Open circuit voltage calculation for a commercialized Zinc-Air battery (Howard, et al., 2015)

Electrode	Reaction	Potential	ΔG^0 (kJ/mol)
Anode	$Zn + 4OH^- \rightleftharpoons Zn(OH)_4^{-2} + 2e^-$		
Anode	$Zn(OH)_4^- \rightleftharpoons ZnO + H_2O + 2OH^-$		
Overall Anode	$Zn + 2OH^- \rightleftharpoons ZnO + H_2O + 2e^-$	$V_A^0 = -1.260$	-243
Cathode	$\frac{1}{2}O_2 + H_2O + 2e^- \rightleftharpoons 2OH^-$	$V_C^0 = +0.401$	-155
Overall	$\frac{1}{2}O_2 + Zn \rightleftharpoons ZnO$	$V^0 = V_c^0 - V_a^0$ $V^0 = 1.6661\ V$	-321

Furthermore, the calculation for the electrochemical equivalents, capacity, service life, and gravimetric energy densities were all performed as well to display the positive motivations of

investigating the gallium-air cell. The theoretical electrochemical equivalent is defined as the energy capacity or available ampere-hours that is available per unit mass of material. Equation 3 is used where E_Q is the electrochemical equivalent. In comparison, the capacity, *Q*, is situation specific, where a known mass of active material is used in the system determines the capacity based on the known mass and electrochemical equivalent. Furthermore, the discharge time, *t*, is determined by the capacity and the discharge current. Finally, the gravimetric energy density is similar to electrochemical equivalent, but instead, it is the amount of energy that can be obtained when one gram of active material, as in our test battery, is discharged. As a result, metal-air batteries generally have some of the highest gravimetric energy densities as one of the active materials is air, which has very little weight compared to other electrode materials. Assuming 1.20 grams of active material with a discharge rate of 1.0 mA, all of the defined values between the gallium-air cell and a commercial zinc-air battery are tabulated in Table 5 and their subsequent equations are shown below (Howard, et al., 2015).

$$\mathrm{E_Q}\left[\frac{\mathrm{Ah}}{\mathrm{g}}\right] = \frac{\mathrm{nF}}{3600\times \mathrm{Molecule\ Weight_{anode}}} \tag{3}$$

$$\mathrm{Q[Ah]} = \mathrm{E_q}\left[\frac{\mathrm{Ah}}{\mathrm{g}}\right]\mathrm{m_{active\ material}[g]} \tag{4}$$

$$\mathrm{t[h]} = \frac{\mathrm{Q\ [mAh]}}{\mathrm{Discharge\ Rate\ [mA]}} \tag{5}$$

$$\mathrm{Gravimetric\ Energy\ Density}\left[\frac{\mathrm{Wh}}{\mathrm{kg}}\right] = \mathrm{V_o[V]} \times \mathrm{E_{Q,anode}}\left[\frac{\mathrm{Ah}}{\mathrm{g}}\right] * 1000\left[\frac{\mathrm{g}}{\mathrm{kg}}\right] \tag{6}$$

Table 5: Theoretical electrochemical equivalents, capacities, discharge times, and gravimetric energy densities of zinc-air and gallium-air batteries (Howard, et al., 2015)

System	E_Q (mAh/g)	Q (mAh)	t (hours)	Gravimetric Energy Density (Wh/kg)
Zinc-Air	820	984	984	1,361
Gallium Air (Hydroxide)	1150	1,384	1,384	1,895
Gallium Air (Oxide)	1150	1,384	1,384	1,989

As a result, it is clear that from the calculation of Howard, et al. (2015) that there is substantial motivation in optimizing the gallium-air cell, as it is superior in the theoretical electrochemical properties (Howard, et al., 2015).

2.7.3: Electrolyte

The electrolyte plays an important role in the performance of metal-air batteries. Metals used for the anode (Zn, Li, Mg, and Al) are very reactive. This results in high amounts of corrosion leading to alkaline solutions being adopted for aqueous electrolytes for metal-air batteries. In addition, the oxygen-reduction reaction (ORR) in alkaline electrolyte is more suited due to better kinetics and lower overpotentials (Cheng & Chen, 2011). The ORR pathway consists of four main steps: hydroxide displacement on the surface, creation of peroxide, oxide formation, and hydroxide regeneration. From some studies, it was found that the hydroxide displacement and regeneration is the limiting factor for the ORR in alkaline electrolytes in metal-air batteries (Cheng & Chen, 2011).

$$O_2 + 2H_2O + 4e^- \rightarrow 4OH^{-1} \quad (7)$$

$$O_2 + H_2O + 2e^- \rightarrow HO_2^- \, OH^{-1} \quad (8)$$

$$H_2O + HO_2^- + 2e^- \rightarrow 3OH^{-1} \quad (9)$$

Aqueous electrolyte is often used since it is relatively inexpensive, easily accessible, and has high ionic conductivity. For metal-air batteries using an aqueous electrolyte, the O_2 is reduced to OH^- that dissolves into the electrolyte. An issue arises with alkaline electrolytes, however, because of the formation of carbonate (CO_2 and OH^- reacting to make carbon-based and water). Since carbonates are insoluble in the electrolyte, the carbonate particles can block the pores in the separator, limiting channels for the ions to travel between cathode and anode.

$$2KOH + CO_2 \rightarrow K_2CO_3 + H_2O \quad (4)$$

To prevent this problem, the CO_2 must be eliminated from the system. This could be done by providing purified air with no CO_2 present or use a membrane that is selective to O_2 only. Another method would involve circulating the electrolyte to prevent any carbonate from accumulating on the separator. This could prolong the discharge duration compared to if the electrolyte is stationary (Cheng & Chen, 2011).

2.7.4: Gas Diffusion Layer

Metal-air batteries deal with a three-phase system where the reaction occurs at the liquid-gas-solid interface. Oxygen solubility in an aqueous electrolyte is low and a catalyst is needed to aid the reduction reaction. Choosing the correct catalyst for the reaction is an art due to the ORR pathways and mechanisms. The ORR mechanisms differ even within the same catalyst since it is

structure-sensitive. This is because the crystallographic structure along with the binding energy affect the oxygen adsorption on the active sites, which results in how the oxygen interaction with the catalyst surface (Cheng & Chen, 2011).

The catalyst influences and dictates the energy conversion, but also contributes to the high costs. A wide range of materials can be utilized as the catalyst, with noble metals (like platinum) being the most popular. Metal alloys, transition-metal oxides, and metal macrocyclic compounds are also used as alternatives for lower costs. Since the reaction takes place at the three-phase interface, the battery setup needs to allow air to diffuse throughout the system so that the electrolyte can absorb it from the catalyst surface. Therefore, the catalyst side of the gas diffusion layer must be hydrophilic to attract the electrolyte while the gas side should be hydrophobic. Commercially, the catalyst side often has the hydrophilic additives and the gas side is coated with paraffin wax or Teflon to repel aqueous components (Cheng & Chen, 2011).

2.7.5: Platinum/Carbon

Platinum (Pt) has been known for oxygen-evolution reaction and been implemented to both batteries and fuel cells. However, platinum is very expensive, so its cost prevents the technology from being widely used. Therefore, much research has been devoted to discovering an alternative in place of the platinum. Despite its high price though, platinum is still of great interest because of its high stability and activity compared to other materials. Since it is commonly used, Pt availability is decreasing and so research has been focused on improving its activity and properties while minimizing its loading. This results in manipulating the size and shape of Pt-based nanoparticles to obtain high surface area while still maintaining the efficiency. One possible alternative is alloying Pt with other inexpensive noble metals or transition metals to produce a cheaper catalyst (Cheng & Chen, 2011).

In order for batteries to be rechargeable, noble metals can be used as the catalyst for both ORR and OER pathways. For alloying, it allows Pt to be combined with another metal that is active for OER to create a bifunctional catalyst. This allows different combinations of metals to provide the desirable performance for discharge and recharge. For example, PtAu/C is a mixture of metals that provide discharge and charge voltage similar to Pt/C. However, others have steered away from the usage of platinum as the catalyst how a variety of consumer products due to the lack of this resource. Researchers are investigating noble, metal-free catalysts for a low cost alternative. One example is carbonaceous materials that can act as either the catalyst supports or catalysts for the reaction. Besides just the low cost, carbon has high wettability, high surface area, good conductivity, and has stability when exposed to extreme conditions. In addition, it can be altered to improve the electrode, such as carbon nanotubes with tungsten carbide, for Pt electrocatalysts for high potential and better current density (Cheng & Chen, 2011).

2.7.6: Manganese Oxide

As mentioned before, transition-metal oxides could also be used as the catalysts for a less expensive option. Manganese oxide has been investigated due to its variable valences and structure that would be suitable for redox electrochemistry as a noble metal-free catalyst. In an alkaline solution, manganese oxide is catalytically active in the ORR pathway. The crystallographic structures and shape do influence how well manganese oxide performs in the reaction. Another method to improve the activity is to combine MnO_2 with other electrocatalytic components. Composites of manganese oxides with noble metals (platinum) or other mixed-valence transition metals have also garnered some interests. Bifunctional catalysts for metal-air is desirable for rechargeability so cobalt and manganese spinels have great potential for air electrodes. The cobalt

and manganese have great catalytic activity and resistance against corrosion in alkaline media. Therefore, manganese-based oxides could be an inexpensive alternative to the platinum-based catalysts that can withstand the harsh alkaline solutions (Cheng & Chen, 2011).

CHAPTER 3: METHODOLOGY

3.1: Design of the Battery

Gallium-air testing was performed with the same modified version of a Li-air Swagelok cell mentioned in Howard, et al. (2015). An expanded conceptual view at the initial version of the baseline cell in shown in Figure 16. See Appendix A-D for the more detailed procedure for battery assembly.

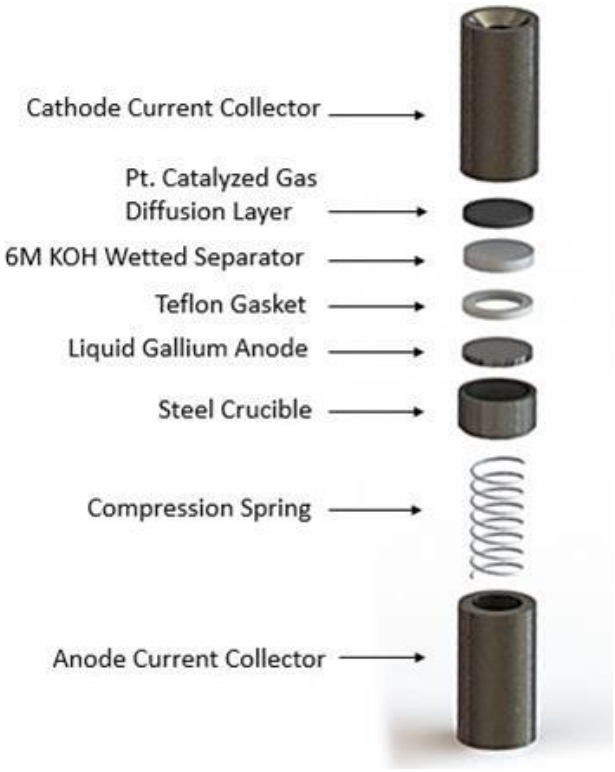

Figure 16: Expanded conceptual view of previous baseline

3.2: Materials

The materials and components used to construct the battery can be sectioned into four categories: structural parts, anode materials, electrolyte separator materials, and cathode materials. The specifics involved with these categories are described below.

3.2.1: Structural Parts

The structural parts for the battery include two current collectors and the casing. The technical specifications, as provided in a previous Major Qualifying Project (MQP) by Howard, et al. (2015) are the following (Figure 16):

- Two stainless steel node current collectors, manufactured by Target Machine
- Stainless steel crucible, machined by WPI Unit Operations Lab
- McCaster Carr 302 Stainless Steel Precision Compression Spring (0.750 in. long, 0.36 in. O.D., 0.026 in. thick wire)
- PTFE Swagelok Tube Fitting with Ferrules, Union, 0.5 in. Tube O.D.

All subsequent testing was conducting using this setup, as shown in Figure 16.

3.2.2: Anode

As a continuation of a prior Major Qualifying Project (Howard, et al., 2015), the decision was made to retain liquid gallium purchased from Alfa Aesar as the chosen anode metal. Gallium, with 99.999 percent, was chosen for its attractive properties such as its non-toxicity, increased reactivity, potential reversibility, self-healing properties, and low melting point (29.77°C) (Howard, et al., 2015). Alternative anode materials were discussed, but resources and time limited options.

3.2.3: Electrolyte Separator

The baseline electrolyte for this battery was a 6 M solution of potassium hydroxide (KOH). Through soaking and capillary action, the electrolyte solution is absorbed into the separator. Here,

the baseline separator is a Zircar woven cloth type ZYK-15 (yttria-stabilized zirconia), with a thickness of 0.012 inches and a porosity of 85 percent (Howard, et al., 2015). In addition to the zirconia cloth separator, alumina cloth and a gelled version of KOH solution were also tested as feasible alternatives. Alterations were made in the electrolyte component in an effort to improve the gallium-air battery performance, both in polarization and discharge durations. Instead of the one separator system conducted in last year's project, it was decided to investigate with two separators soaked in 6 M KOH. This system would increase the amount of KOH in the system and allow it to retain the aqueous solution for an extended time. Another method to increase the amount of KOH was transition from 6 M to 8 M KOH solution. With the two different concentrations of KOH, the team also wanted to determine whether regenerating the electrolyte by resoaking the separators in either KOH solutions or simply water would yield consistent performance and extend the discharge lifetime after each resoak. The reason behind resoaking the separators would be to simulate a flow battery system, where the electrolyte would constantly cycle through the system to prevent carbonation from forming on the separators and limiting performance and lifetime.

Figure 17: Diagram of some alterations made to the electrolyte to improve gallium-air battery performance

A two zirconia cloth separator system was assembled following the same procedure as the one separator system except for a few changes. First, two cut zirconia cloth separator of equal size was soaked in the same 6 M KOH solution for a minimum of 20 minutes. Then, during cell assembly, the second wetted separator was placed on top of the first separator followed by the GDL.

As previously mentioned, a gelled version of the electrolyte solution was also investigated and tested. Polyvinyl alcohol (PVA), the gelling agent, and KOH have been used to make alkaline solid polymer electrolytes. This method would limit the water content in the 6 M KOH electrolyte solution, which is prone to evaporation. A 60:40 ratio of PVA:KOH was chosen based on literature (Palacios, et al., 2003). To make the 60:40 ratio of PVA-KOH, a beaker with deionized water was heated to 80^{o}C using a heat plate. A stir bar provided constant stirring for a homogenous solution. Once the water was heated, 3.0 grams of PVA were added to the beaker and left to mix until no PVA pellets were present. 2.0 grams of KOH were then added into the continuously stirred beaker. After about 15 minutes, the heat was turned off while the stirring continued for roughly five hours. Once the solution was cooled down to room temperature, it was transferred to petri dishes to evaporate off excess water and to form a thin film. During this step, cut zirconia cloth separators were added to the evaporating film. In another petri dish, gallium droplets were added to the PVA-KOH film in one petri dish in an attempt to create a three-dimensional matrix between gallium and electrolyte in the anode compartment, as in a commercial zinc-air cell (Figure 11), compared to the two-dimensional electrochemical interface between the surface of the gallium and the soaked separator, as in the current design.

3.2.4: Cathode

The cathode component consumed in this battery is the ambient air of the testing laboratory. The cathode assembly included a catalyzed gas diffusion layer (GDL), supplied by the Fuel Cell Store. The GDL acted to reduce and evolve oxygen gas from air (Howard, et al., 2015). The baseline GDL material was a platinum-catalyzed carbon paper coated in Teflon. Two different types of carbon paper catalyzed by manganese oxide were also tested briefly with the purpose of determining the battery's rechargeability.

3.3: Electrochemical Cell Set Up and Testing

The gallium-air battery was assembled and tested in the WPI Fuel Cell Laboratory. Approximately 1.2 grams of gallium were melted under a heat lamp, weighed, and placed inside the stainless steel crucible. Next, a Teflon gasket, zirconia cloth separators, and a GDL are manually cut to size using various hole punchers (Figure 16). The Teflon gasket was created using two hole punchers, one to cut the inner diameter hole and the other to cut the outer. The gasket's function is to prevent any leakage of the liquid gallium out of the crucible and into the cathode. The zirconia cloth, cut with a hole puncher, was then soaked in a 10 mL solution of 6 M KOH for approximately 20 minutes to sufficiently wet the separator. In the assembly process, the battery is built from anode to cathode.

When fully assembled, the battery was inverted, attached to a ring stand, and placed under a heat lamp and a temperature probe was placed at the middle of the battery. The cell was inverted to increase the interfacial surface contact between the liquid gallium and the KOH wetted separator. The heat lamp prevents the gallium from solidifying during test runs. For a more detailed look at the process, refer to Appendix D.

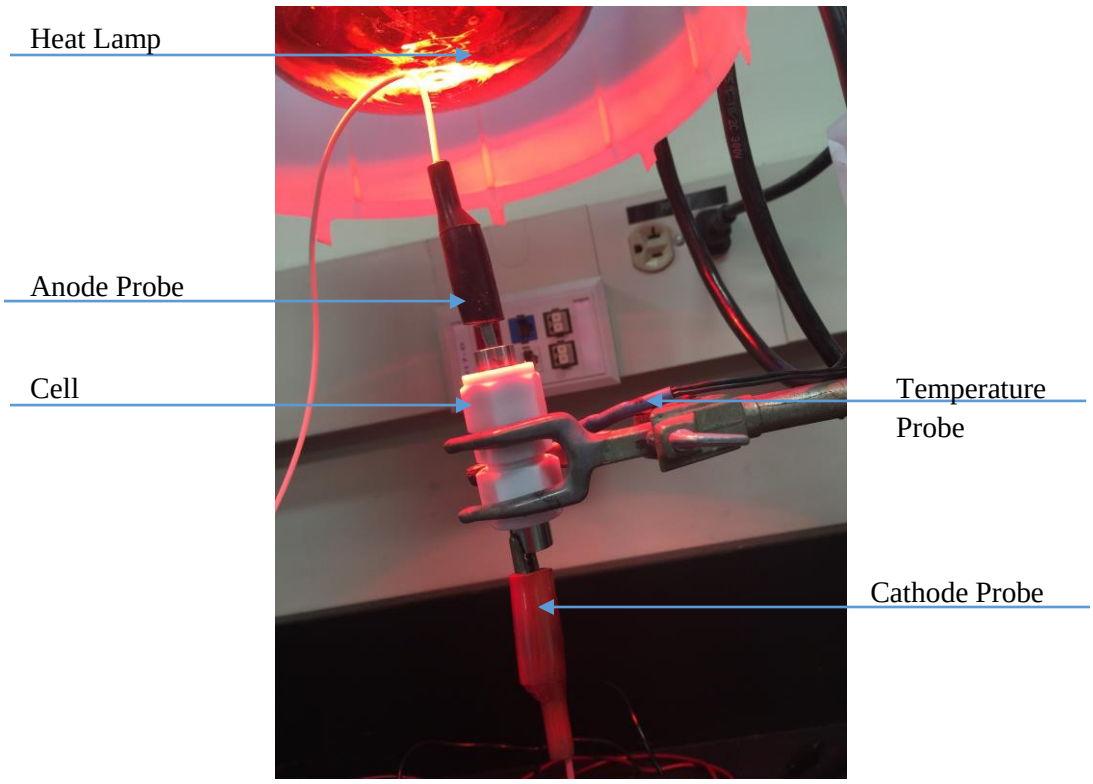

Figure 18: Ring stand and heating lamp setup with inverted cell

3.4: Battery Metric (BA500WIN Setup)

Throughout the testing process, the Battery Metric was used in order run the experiments, as this device controlled the amperage, and monitored voltage, temperature, and time. The battery metric from Howard, et al. (2015) was used for this testing. It is a modified version of the MC2020 model purchased from Battery Metric. This model is specifically customized with the ability to accurately discharge and charge batteries at low currents. The software provided alongside this model was the BA500WIN program, Ver.1.38 (Battery Metric, 2011). This program has the capability of utilizing both manual and automatic control of the voltage, current, and durations of individual tests. The window can be shown below. In the graphing region shown in the figure, the

voltage, in yellow, and current, in blue, displayed the outputs in real time and allowed for tests to be monitored and terminated if necessary.

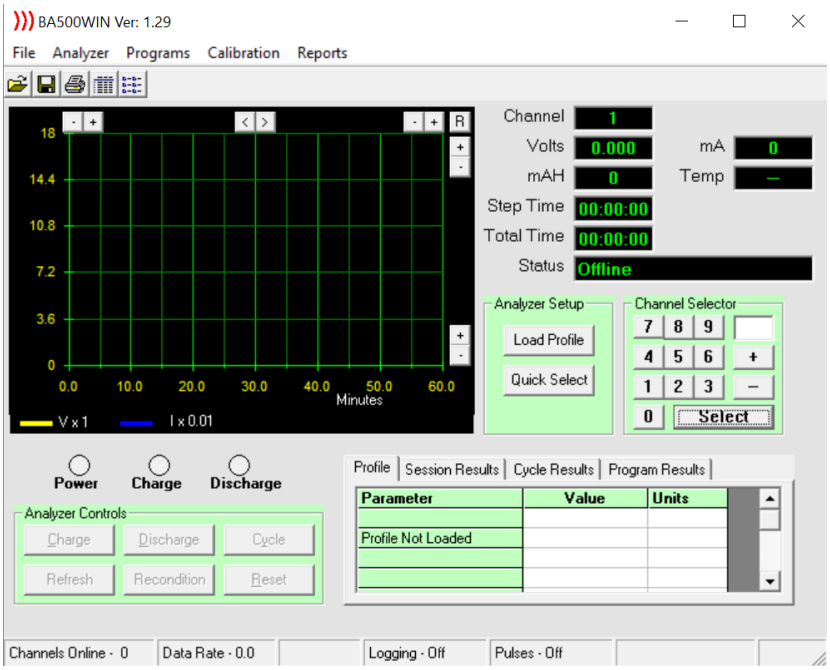

Figure 19: Display of the BA500WIN program

For a majority of the tests, a continuous script was utilized that was constructed using the Program function, as shown in Figure 20. Under "Battery Type," the Nickel-Cadmium option was used in the event that the tests involved attempts in charging the battery cell. For most primary cell purposes, both of these options behave in the same manner and are subjected to similar voltage and currents. Since the gallium system only had one cell, the number "1" was entered into the "No. of Cells", and an estimated capacity of 1,000 mAh, predicted from the previous report, was entered for "Rated Capacity".

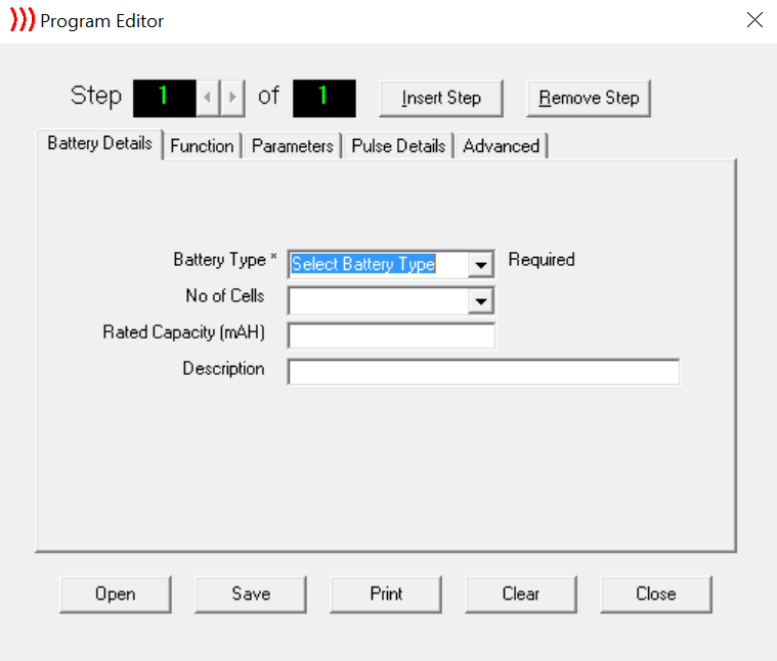

Figure 20: Display of the Program Editor program in BA500WIN

For most of the experiments, the script that was utilized contained a twenty-minute open-circuit voltage hold and then a galvanostaircase polarization curve that measured currents in increasing increments of 0.1 mA between 0 mA and 7.5 mA and then in increments of 0.5 mA until the current reached 15 mA. Each current point was held for 20 seconds, with a discharge cut-off voltage of 0.1 V, so that the mass-transport regime could be further examined with each tested current density. These values were entered into the program as shown in below.

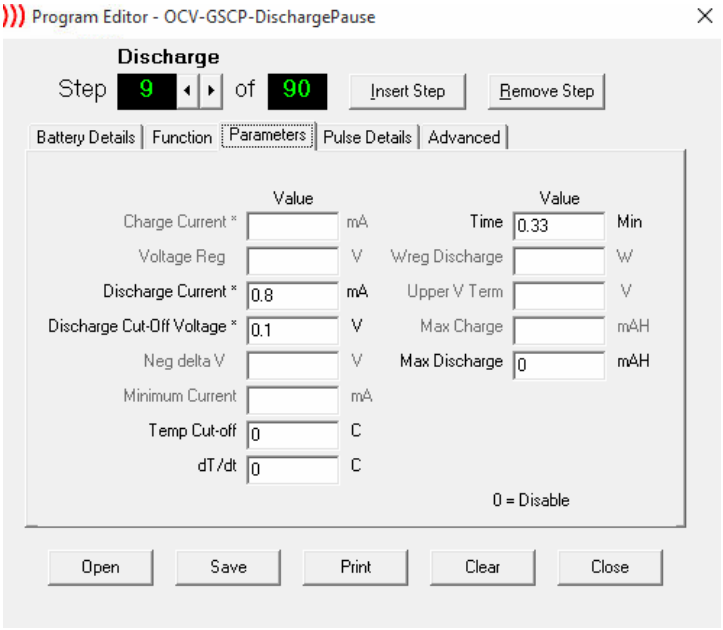

Figure 21: Display of the input parameters of the Program Editor program in BA500WIN

Once this polarization test was completed, the script called for a fifteen-minute pause for the system to recover and stabilize and was then subjected to a constant current draw for the discharge curve. Depending on the test, these constant current outputs ranged between 0.5 mA to 3.0 mA. The final step of this script was another pause so that the difference in the open-circuit voltages could be determined after the length of the test.

For the charging experiments that were attempted, the initial OCV, polarization, and full discharge were performed congruently with the prior procedure. Once the cell had ceased to discharge, a short pause (10 minutes) ensued, followed by a 0.5 mA charge step for 60 minutes. Another short pause step was entered and the cycle was completed with a final 0.5 mA discharge step for 60 minutes. The cell underwent this cycle two additional times. The final discharge lasted until the cell failed to hold a voltage greater than 0.1 V.

CHAPTER 4: RESULTS

Most of the conditions and setup of the gallium-air battery were based on previous work done last year on A New Liquid Metal-Air Battery project (Howard, et al., 2015). Initially, their methodology was adopted in order to compare the results from the previous work. Changes and adaptations to the baseline battery configuration were subsequently made as conclusions were drawn from analyzing data. The main three objectives for this project were:

- Reproducing the results of the previous project to ensure the methodology is consistent for comparing data and easy to replicate
- Improving the performance of the gallium-air battery by altering the physical component of the battery, like the electrolyte layer or the GDL and cathode layer
- Investigating gallium-air rechargeability once the optimal conditions were determined

4.1: Motivation for Developing Gallium-Air Batteries

As discussed in Chapter 2, the energy needs are continuously growing and the energy storage capacity must also follow this trend if the world is to rely more on renewable energy. However, even if energy storage devices improve in capacity, they must also simultaneously improve in their ability to release large amounts of energy safely. Towards these goals, the performance of the gallium-air battery was investigated and also compared to the traditional zinc-air button cell. The zinc-air cell is the current, commercial version of the metal-air battery technology that this project is trying to improve upon.

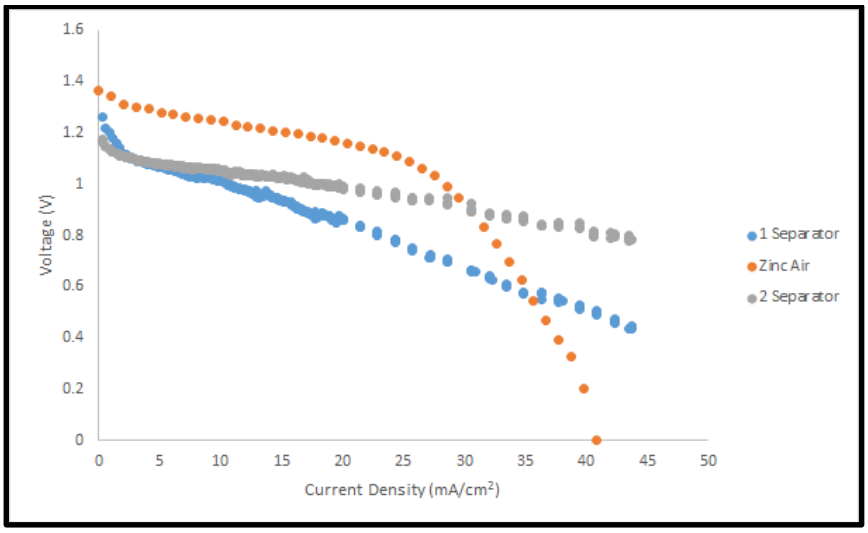

Figure 22: Polarization Curves comparing different configurations of the gallium-air battery to a traditional zinc-air battery

In Figure 22, the polarization curves of the original baseline gallium-air battery, the new baseline gallium-air battery, and the traditional zinc-air battery are shown. To get a fair comparison, the Duracell 675 zinc-air battery was used because the size and surface area of the active area was comparable to that of the gallium-air battery. Upon taking the polarization curves of the three systems, it is evident that for most current densities, the zinc-air battery is superior in voltage and performance, as it can deliver higher potential at the same current densities of either gallium-air cells. On the other hand though, it is important to note that in the zinc-air system that there is a very sharp decline in voltage as the system is approaching the mass-transfer limitation regime and the electrochemical reaction can no longer be sustained, resulting in a loss of voltage. For the zinc-air system, once current density reaches past roughly 25 mA/cm^2, mass-transport limitations arise and voltage begins to decline rapidly. On the other hand, the gallium-air system does not have this mass transfer limitation. This is believed to be the result of the commercial battery design (Figure 11), which involves an anode can with gelled Zinc/KOH mixture. This extends the electrochemical reaction interface significantly, unlike the gallium-air cell, which is

two-dimensional interaction being limited to the gallium/separator interface. This can explain bulk higher performance initially and the sharp, subsequent drop. Although our system, in both cases shown in Figure 22, does not perform as well as the zinc-air for lower current densities, the gallium-air cell does continue to perform exceptionally well in the higher current density regimes, as it can easily reach current densities of up to 45 mA/cm^2 without ever reaching mass transport limitations. Although the voltage at these high current densities are still somewhat lower, there is no sharp drop characteristic of mass transport limitation. Due to these results, there is motivation to discover the conditions that can be optimized so that these overpotentials are even lower so that power output can be increased. It may be theorized, based on these results, that the kinetics of the gallium-air battery are faster and the performance might be improved by a three-dimensional design that resembles a zinc-air battery.

4.2: Reproducibility of Results

The project conducted last year (Howard, et al., 2015) had the baseline conditions for discharge tests shown in the table below.

Table 6: Baseline conditions for discharge tests (Howard, et al., 2015)

Electrolyte	33.6 wt.% KOH (6 M)
Separator Material	1 Zirconia Cloth
Heat Source	Heating Lamp
Discharge Current	0.5 mA
Current Density	1.41 mA/cm^2
Cell Orientation	Cathode facing downward (inverted)
Ambient Temperature	40-50^oC

We maintained these operating conditions initially in order to ensure the methodology was consistent. Based from last year, the average test would last for 5 hours, while the longest duration was over 16 hours. The large variation in discharge duration perhaps resulted from assembly inconsistencies during different runs. For the baseline test and comparison with Howard, et al. (2015), a 12 hour discharge of gallium-air battery at 40°C was achieved. The temperature was about 10 degrees higher than the melting point of gallium to ensure the gallium maintain in liquid phase during the experiment (Howard, et al., 2015). This was also an experiment that was run last year with a one separator system with 6 M KOH at 40°C, as shown in Figure 23.

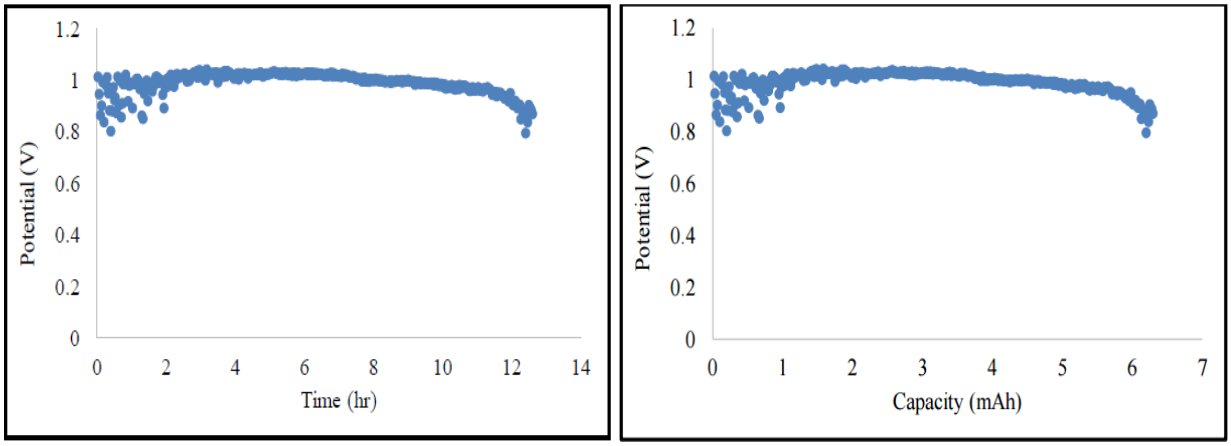

Figure 23: Gallium-air battery discharge curve, one separator system at 40°C (left) and voltage vs. capacity at 40°C (right) (Howard, et al., 2015)

Although the beginning of the test showed some fluctuation in voltage, the discharge curve was relatively constant throughout the period of 12.6 hours. When comparing the potential (voltage) with the capacity (mAh), roughly 6 mAh for that particular experiment, the two plots are shown in Figure 23 (Howard, et al., 2015).

This is comparable to the results gathered this year for the same conditions. The left graph in Figure 24 displays the discharge duration for the reproduced, one separator system at the same temperature (40°C) and concentration of KOH (6 M). For that particular run, the experiment lasted

for about 10 hours with a relatively smooth discharge curve. The capacity of the gallium-air battery was also investigated and is shown on the right graph in Figure 24. The capacity was roughly 5.3 mAh, which was slightly lower than last year's test. However, the results' close comparison demonstrated that the methodology and assembly was consistent with the previous year. This forwarded the basis of further experimentation to be conducted to improve the performance of the gallium-air battery by altering the electrolyte or the cathode components of the cell.

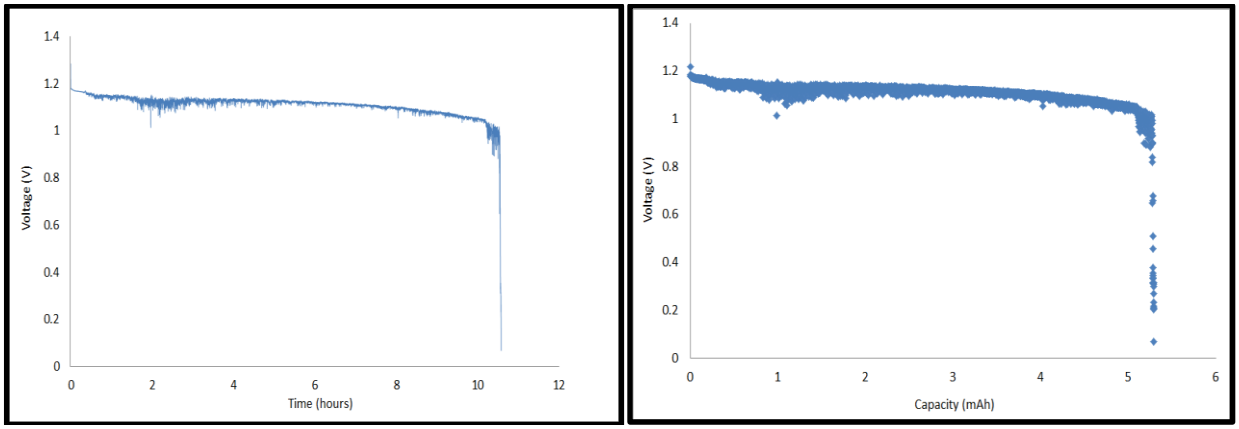

Figure 24: Gallium-air battery discharge curve, one separator system at 40°C (left) and voltage vs. capacity at 40°C (right) (Howard, et al., 2015)

4.3 Optimization of the Gallium-Air Battery

To improve the discharge performance of the battery limited presumably by either drying or carbonation of the electrolyte, many alterations to the electrolyte components were tested. The trials involved gelling the KOH using PVA around the separator and mixing gallium droplets into KOH gelled to simulate the three-dimension matrix for the reaction to occur, to mimic the configuration of the Zn-air. These experiments proved inconsistent and inconclusive, not providing stable and long discharge duration. Alumina cloth, as a replacement for zirconia cloth, also showed little improvement. However, when two separators dipped in 6 M KOH were used for the electrolyte component, longer discharge durations of about 25 hours were consistently achievable.

Discharges of one separator cells did not exceed 10-12 hours. When compared, the two separator cells more than doubled the previous baseline's best, as shown in Figure 25.

The reason for adding another KOH soaked separator into the battery was to increase the amount of KOH in the system. A postmortem analysis of a single separator cell after its discharge showed that the separator was completely dry. Adding a second soaked separator served to increase the amount of water and KOH in the system to prevent it from drying out. This ended up significantly extending the battery's life, as shown in Figure 25.

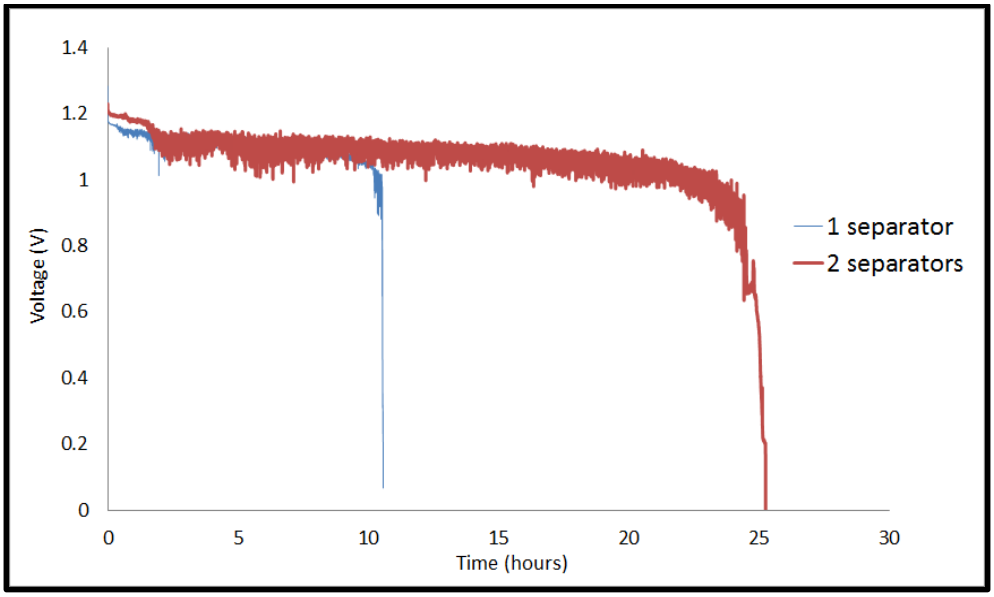

Figure 25: Two separators discharge duration compared to one separator

After repeated and comprehensive testing, thus a new, updated baseline was established to compare against further alterations, shown in Table 7. All subsequent tests were performed with two separators instead of one.

Table 7: Updated baseline for the gallium-air battery

Electrolyte	33.6 wt.% KOH (6 M)
Separator	2 Zirconia Cloths
Heat Source	Heating Lamp
Discharge Current	0.5 mA
Current Density	1.41 mA/cm^2
Cell Orientation	Cathode facing downward (inverted)
Ambient Temperature	~50^{o}C

The effect of temperature on the performance and discharge characteristics of the Ga-air battery was evaluated. These are competing effects, thus anode and cathode kinetics, as well as electrolyte conductivity, improved with temperature. On the other hand, drying of the electrolyte would be expedited. As indicated in literature on the performance and discharge capability of metal-air batteries, as temperature increases the discharge duration decreases (Zhou, 2014). The results of the change of temperature on discharge performance from last year's project (Howard, et al., 2015), is shown in Figure 26.

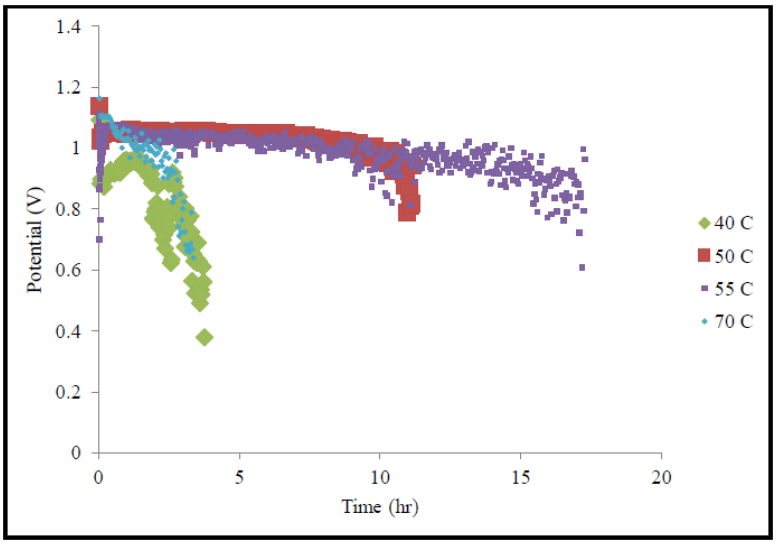

Figure 26: Discharge curves from last year results for gallium-air with one separator system at temperature range from 40°C to 70°C (Howard, et al., 2015)

Based on this plot, the optimum temperature is 55^{o}C, with a discharge duration of about 17 hours long. At lower and higher temperatures, like 40^{o}C and 70^{o}C, the discharge lasted for about 5 hours. As for the rapid decline in duration at 70^{o}C, it is imagined that the higher temperature dried the separator more quickly, evaporating the aqueous alkaline solution. Without the presence of KOH solution in the system, the reaction could not (Howard, et al., 2015).

This trend was generally observed, even with our improved two separator system when the temperature was varied, shown in Figure 27. The temperature with the longest duration is about 50^{o}C for about 27 hours. Surprisingly, the next long duration occurred at 40^{o}C for about 25 hours as compared with last year that achieved only about 5 hours. The difference between the two tests besides the number of zirconia cloths in the system could be the phase of the gallium in the anode. In the previous experiments, it is hypothesized that the gallium was in the solid state during the experiment since the temperature inside the cell was lower than 40^{o}C, due to the probe placement, while the gallium remained in liquid phase when disassembled in our experiments ran this year. Therefore the gallium had more contact with the zirconia cloth surface area (where the 6 M KOH electrolyte was). At lower temperature, the aqueous alkaline solution was not prone to evaporation, which extended the discharge duration greatly.

A similar trend from last year was observed with our two separators system at the higher temperatures. In the temperature range of 60^{o}C to 70^{o}C, as the discharge duration decreased as temperature was increased. For the temperature at 70^{o}C, the duration of the test lasted roughly 12.5 hours, which is about half the discharge period when compared to other temperatures. This phenomenon could be explained due to the evaporation of the aqueous alkaline solution, resulting in the separators drying out. Without the liquid KOH solution in the system, the reaction between gallium and hydroxide would not occur.

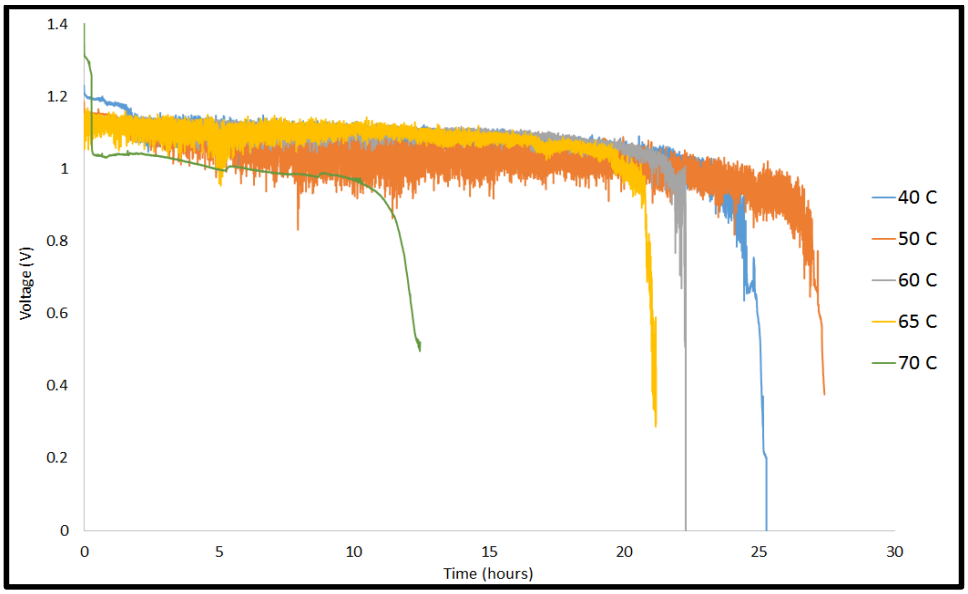

Figure 27: Discharge curves for gallium-air with two separators system at temperature range from 40°C to 70°C

Besides the discharge curve, the polarization curve was also examined to observe the gallium-air performance as a function of temperature and is shown in Figure 28. Since polarization curves were obtained before each discharge experiment, the performance of the battery could be observed at different temperatures. As seen in the Figure 28, 40^{o}C performed very well along with 50^{o}C. Temperatures of 60^{o} and 65^{o}C were where the polarization curves did slightly worse. For 70^{o}C, the performance decreased drastically with inconsistencies in voltage readings that did not result in the smoother trend as previous tests. At that high temperature, the system was unstable and resulted in the fluctuation of voltage during the polarization test. This corresponded with the short discharge duration of about 12.5 hours at the high temperature. The general trend appears to indicate that the lower temperatures (40^{o}C to 60^{o}C) result in better performance than the higher temperatures (65^{o}C to 70^{o}C).

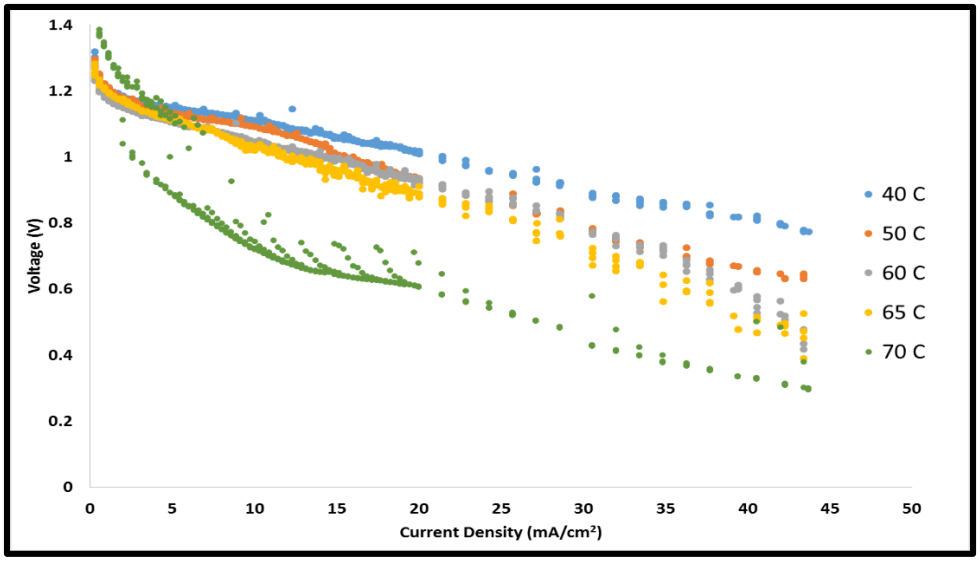

Figure 28: Polarization curves for two separators system at temperature range from 40°C to 70°C

In addition to conducting the temperature study, another investigation was carried out to identify the limiting factor, or the variable that consistently caused the cell to stop discharging, despite high theoretical energy densities and adequate availability of gallium. Based from the temperature effect on both the one and two separators systems, it was observed that very short discharge times resulted for high temperature of 70°C. Two hypotheses these data proposed were: 1.) the consumption of KOH as the gallium reacted with the hydroxide, or via carbonation with carbon dioxide in the air, and 2.) evaporation of water from the aqueous alkaline solution, as shown schematically in Figure 29.

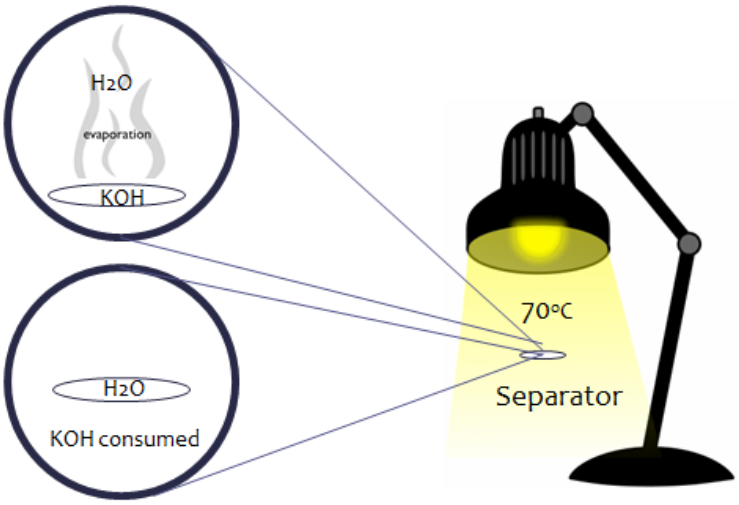

Figure 29: The two possible hypotheses for shortage of discharge performance

To test the first hypothesis involving the consumption of KOH, a baseline cell was run at normal operating conditions until the voltage could no longer be maintained. At this point, the cell was disassembled, and the separators were soaked in the potassium hydroxide solution again and the cell was reassembled using the same materials. From this procedure, the results generated are shown in Figure 30.

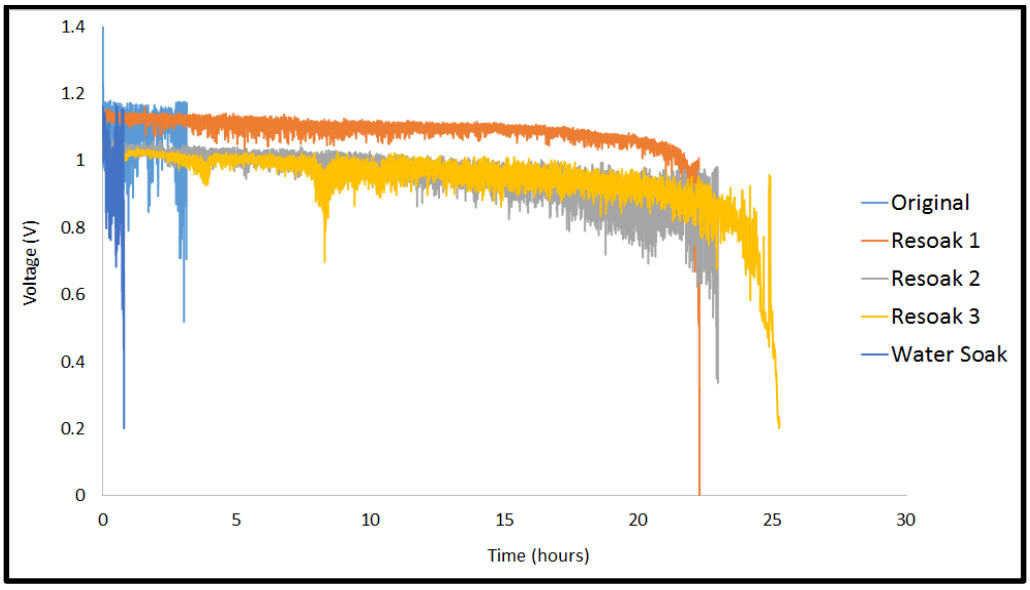

Figure 30: Discharge curves for gallium-air with two separators system where the separators were subjected to multiple KOH soaks.

From the results shown in Figure 30, it can be easily ascertained that, as long as the integrity of the separators was not compromised, multiple KOH solution soaks of the two separators leads to comparable discharge times. However, it can also be seen that over time, that there are more overpotential losses associated with the system as the average discharge voltage in subsequent tests is identifiably lower than the first initial tests. This can also be seen in Figure 31, which displays the polarization curves of each of these experiments. In these plots, it can be seen that with each time that the separators were resoaked in the KOH solution, the polarization performance of the system worsened considerably with a drop of roughly 0.4 volts between the first polarization curve and the final (Resoak 3) at comparable current densities.

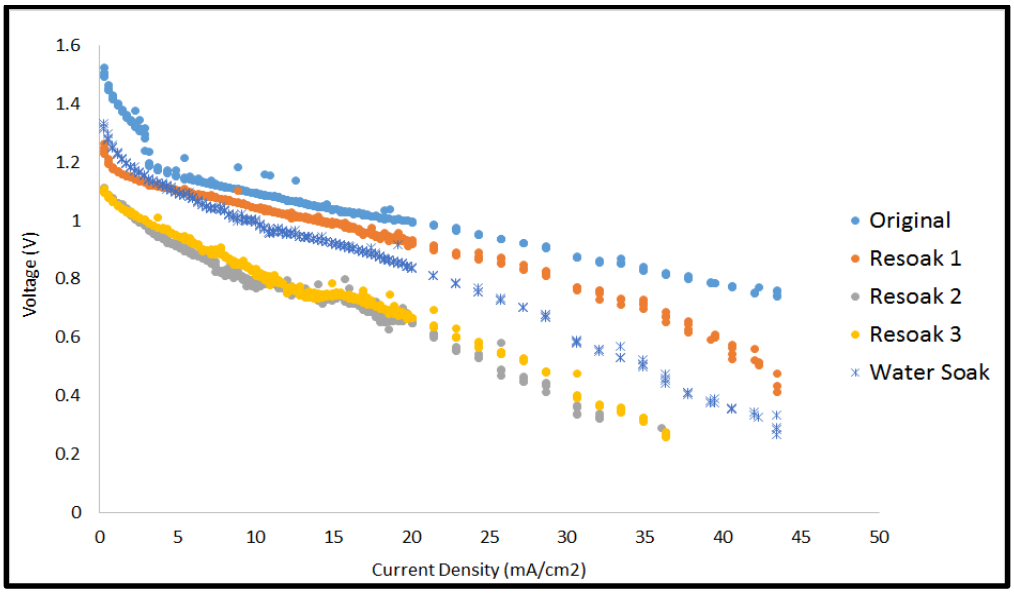

Figure 31: Polarization curve for each resoaking at 6 M KOH

Based on these electrolyte regenerating experiments, it led to the hypotheses that hydroxide is getting consumed during the reaction, either with gallium to generate charge or with carbon dioxide in the surrounding air to form potassium carbonate. To further investigate if the hydroxide

was being consumed, the amount of hydroxide was increased by raising the concentration of KOH to 8 M instead of 6 M. The temperature investigation for 8 M KOH is shown in Figure 32.

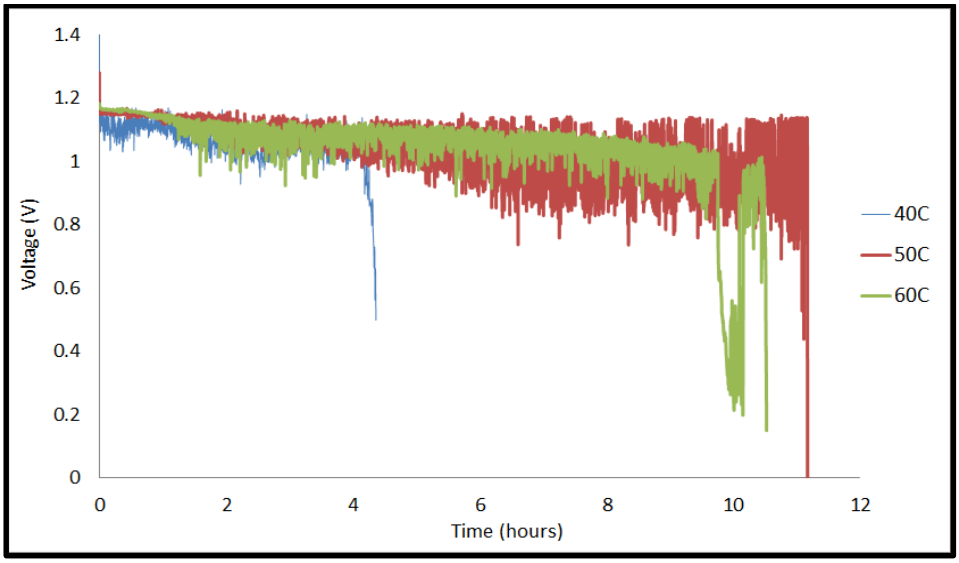

Figure 32: Temperature profile for 8 M KOH at variation of temperatures with two separators

Similar trends were observed for the 8 M KOH experiments as the 6 M KOH system where the best performing temperature is around 50°C with a discharge duration of about 11 hours. The low temperature, 40°C, did not last very long and ended around 4 hours. The higher temperature (60°C) lasted roughly 10 hours with noisy throughout the experiment. The polarization curves at those temperature were also investigated, shown in Figure 32. The performance at 60°C was better than the test at 50°C. For the 40°C experiment, the polarization curve was unstable with fluctuations in potential as the current density was increased. This could explain the reason for the short discharge period that it experienced.

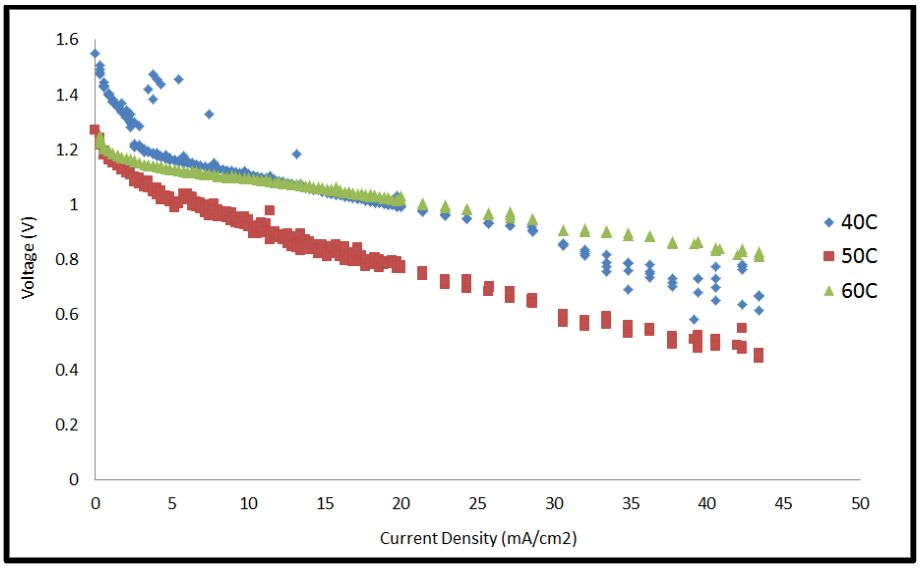

Figure 33: Polarization curves for 8 M KOH system at variation of temperature with two separators

Interestingly, the 8 M KOH did not perform as well neither in polarization nor in discharge experiments as the 6 M KOH even when two separators were used to prevent evaporation of the electrolyte. One possible reason for the lack of good performance in 8 M KOH may be due to the saturation of KOH. This could result in the lack of aqueous alkaline electrolyte and resulted in a shorter discharge time. Based upon this study, 6 M KOH was found to be the optimal concentration of electrolyte that should be used for better polarization performance along with longer duration of discharge.

4.4: Investigating Feasibility of Recharging

In order to achieve the future goal of developing an energy storage system, the battery must be able to successfully recharge after discharging all the energy it has stored the previous day. To gain an initial understanding of the current baseline's recharge performance, tests were conducted with discharge-recharge cycles and were compared against a commercially available nickel-metal

hydride (NiMH) battery (Figures 34 and 35). The gallium-air battery was unable to hold the charge with a current of 0.25 mA while the NiMH battery performed significantly better at a current of 50 mA. A potential reason for this is that platinum is an effective catalyst for electrolysis of any water present above 1.2 V. Alternatives to platinum-catalyzed GDL were researched and manganese oxide (MnO_2) was tested to see if that could serve as a better catalyst for recharging.

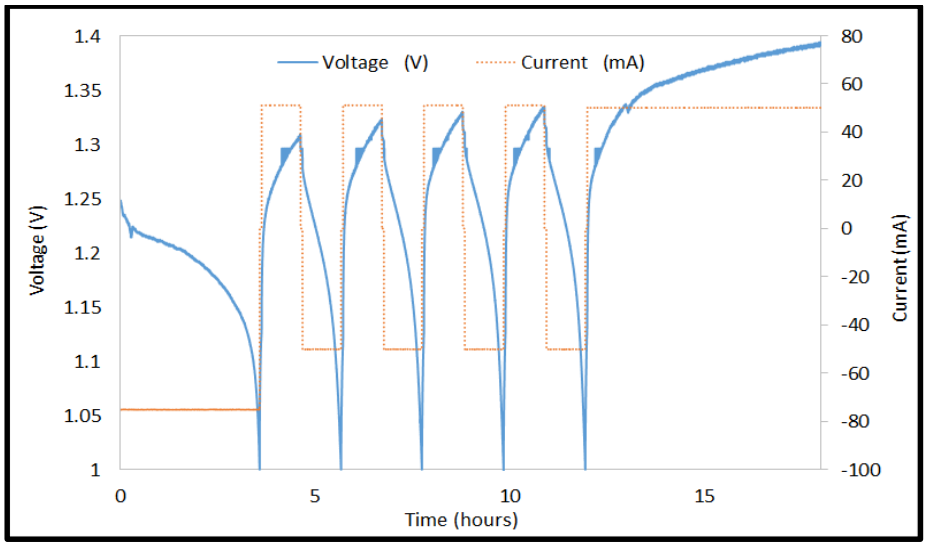

Figure 34: Charge/Discharge Cycles for Commercial NiMH battery

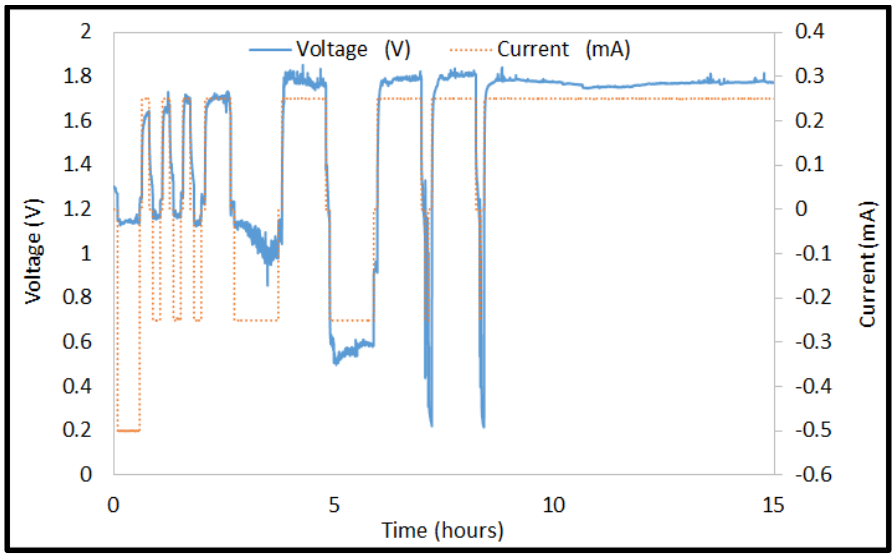

Figure 35: Charge Cycles for Pt-Catalyzed GDL battery

Two different MnO_2-catalyzed carbon papers were thus chosen. However, results were similar to those achieved during the Pt-catalyzed GDL tests, where barely any of the recharge held. Unfortunately, these data might not be completely representative of the cell's actual potential. It was theorized that the lack of rechargeability was due to reaching the potential of water electrolysis. This can be overcome by removing the water from the system through the use of a water-free electrolyte layer. However, this aspect needs significantly more investigation to be deemed conclusive.

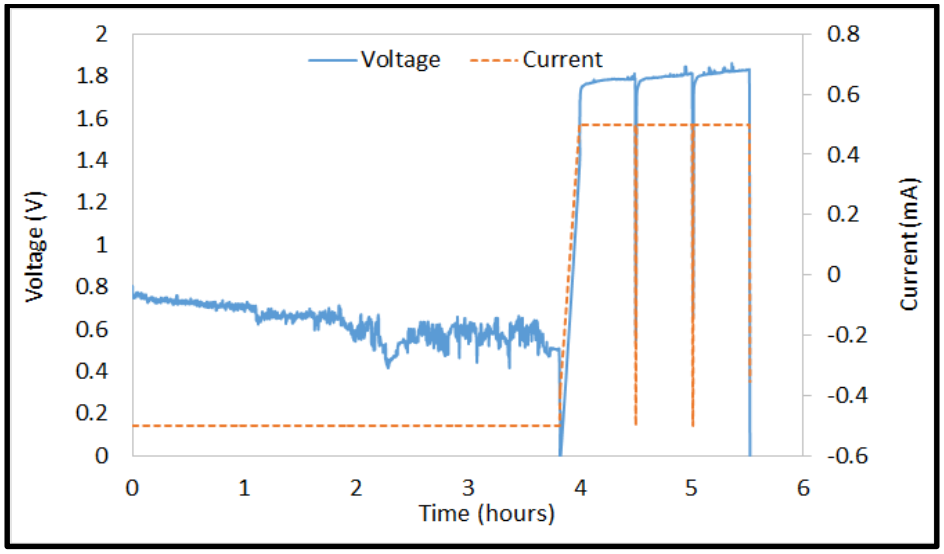

Figure 36: Recharge Cycles for MnO2 GDL battery

CHAPTER 5: CONCLUSIONS AND RECOMMENDATIONS

5.1: Conclusions

Building off previously conducted research on the liquid gallium-air battery (Howard, et al., 2015), significant progress was made. After diligent testing, a number of conclusions were drawn in an effort to improve both the battery's performance and discharge duration. When compared to commercial zinc-air battery, the liquid gallium-air battery performs better at higher current densities that are desirable for grid-wide energy storage. In an effort to optimize the battery, alterations were focused on the electrolyte layer. These alteration include running the cell with alumina cloth, gelled PVA/KOH, increasing KOH concentration, and two KOH soaked zirconia cloth separators. Following these experiments, the two zirconia cloth separators exhibited superior performance, with double the discharge duration. In an attempt to continue improvement of the electrolyte layer, different concentrations of the alkaline solution were tested. Between the options of 6 M and 8 M, 6 M provided better performance. The next step was determining the optimal run temperature for the system. When tested between 40^{o}C and 70^{o}C, at 5-10 degree intervals, performance peaked at 50^{o}C. Through the resoaking process with the zirconia cloth, the hydroxide was determined as a critical limiting component of the reaction. This also revealed that carbonation might be the key reason that limits the performance and discharge duration.

$$2KOH + CO_2 \rightarrow K_2CO_3 + H_2O$$

The amalgamation of these conclusions culminated in a new baseline that significantly improved on the initial design and research of Howard, et al. (2015).

5.2: Recommendations for Future Work

As a result of the conclusions that were drawn, a series of recommendations are given to further optimize and improve the liquid gallium-air battery. The first of these recommendations is to adopt a new configuration that mimics that of a flow battery where the liquid gallium and the alkaline electrolyte are continuously circulated throughout operation. This is suggested because this could reduce any film formation of gallium oxide on the interface between the two different phases and would prevent buildup of any potassium carbonate in the separator, potentially allowing for larger discharge durations. The following schematic is provided as a reference for a potential setup for the proposed flow design. Some important factors that should be taken into consideration with this design is the flow rate of the potassium hydroxide, as it does have to flow through the fragile zirconia cloth separator. High flow rates with a pump could shear the separator. Finally, this system would require two separate pumps, as the two liquid solutions would have to be continuously circulated.

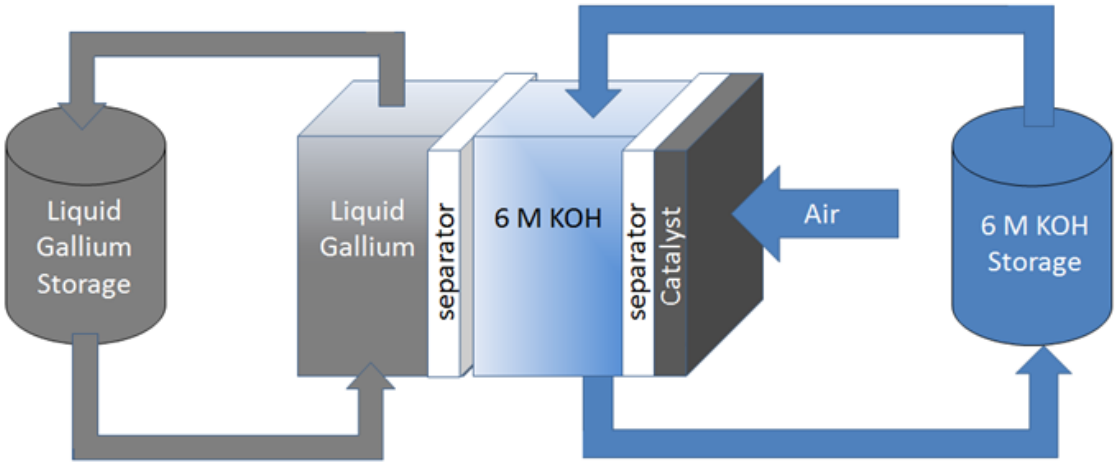

Figure 37: Possible configuration of the gallium-air battery incorporating the flow battery schematic

Another suggestion would be to further investigate commercialized MnO_2 gas diffusion layers in place of the platinum catalyst. Based on literature, manganese oxide is an inexpensive

and efficient alternative for the ORR reaction. This would significantly lower the cost for the gallium-air battery, making it more appealing to be utilized widely. Manganese oxide also shows potential to have recharging capabilities, making it a potential candidate for the grid-scale energy storage since it would be able to store and release excess energy on demand.

In terms of the electrolyte component, ionic liquid could be a potential option to replace the aqueous potassium hydroxide electrolyte to avoid water for a rechargeable cell. Aqueous alkaline electrolyte is also sensitive to the temperature fluctuation and prone to evaporation over time at high temperatures. Since there is no water content in the ionic liquid, it would avoid that issue. This could extend the discharge durations and performance of the gallium-air battery. Further, it could allow recharging. However, ionic liquids require very higher temperatures.

Since gallium is rarely used in electrochemical cells, little is known about the interactions and reactions that are occurring in the different layers in the liquid gallium-air battery. As a result, another recommendation would be to perform a series of surface characterization techniques on both spent separators and gas diffusion layers. This is because the primary gallium reaction is still unclear, and it is not known if the oxide formation or the hydroxide formation dominates the cell performance. As a result, further studies, such as x-ray diffraction or scanning electron microscopy are recommended as tools to analytically detect the compounds found on these interfaces and better understand how exposure to electrochemical reactions can alter the surface morphologies of these components as well.

Initial efforts have led to the conclusion that with the current materials and equipment that the liquid gallium-air battery has poor recharging capabilities. However, this does not mean gallium should be excluded as a possible contender for grid-wide energy storage, especially if the setup adopts a flow battery configuration. Once the primary reaction is known and the final product

in the anode is determined, it is recommended that a method of chemical regeneration of gallium from that product be researched. This would still allow for the regeneration of the gallium, making it possible for the same active material to be used again after some processing. In the flow battery configuration, this is highly practical as the gallium would be separate from the power-producing stack. This means that the gallium tank could be isolated, regenerated back into pure gallium, and then reintroduced into the system to continue releasing energy.

WORKS CITED

Ambri. (2016). Storing Electricity for Our Future [Brochure]. Boston, MA:

Battery Metric. (2011). BA500 Series Battery Analyzers. Retrieved April 25, 2016, from http://batterymetric.com/wp-content/uploads/2014/01/ba500manual.pdf

Bouhafs, F., Mackay, M., & Merabti, M. (2014). Communication Challenges and Solutions in the Smart Grid. Springer.

Cheng, F., & Chen, J. (2011). Metal-air batteries: From oxygen reduction electrochemistry to cathode catalysts. *Chem. Soc. Rev.*, 2172-2192. Retrieved February 23, 2016, from http://pubs.rsc.org/en/content/articlehtml/2012/cs/c1cs15228a

Chung, Yonghwa. "Electrochemistry of Gallium". Journal of electrochemical science and technology (2093-8551), 4(1), p.1 (2013).

Crompton, T. R. (1996). *Battery reference book*. Place of publication not identified: SAE International.

Dunn, B., Kamath, H., & Tarascon, J. (2011). Electrical Energy Storage for the Grid: A Battery of Choices. *Science, 334*(6058), 928-935. doi:10.1126/science.1212741

Eastin, L. J. L. (2014). An assessment of the effectiveness of renewable portfolio standards in the united states. Electricity Journal, 27(7), 126-137. doi:10.1016/j.tej.2014.07.010

Energy Storage Association. (n.d.). Pumped Hydroelectric Storage. Retrieved April 10, 2016, from http://energystorage.org/energy-storage/technologies/pumped-hydroelectric-storage

Howard, Tyler Trettel, Merrill, Laura Christine, Johnston, Stephen Patrick, & Datta, Ravindra (2015). *A new liquid metal-air battery*. Worcester, MA: Worcester Polytechnic Institute.

Huggins, R. A., & SpringerLink ebooks - Engineering. (2010).*Energy storage*. New York: Springer. doi:10.1007/978-1-4419-1024-0

IAE. (2014). World Energy Outlook 2014, Executive Summary. International Energy Agency, OECD/IEA, Paris. Retrieved from: http://www.iea.org/Textbase/npsum/WEO2014SUM.pdf

Ibrahim, H., Ilinca, A., & Perron, J. (2008). Energy storage systems—Characteristics and comparisons.*Renewable and Sustainable Energy Reviews, 12*(5), 1221-1250. doi:10.1016/j.rser.2007.01.023

Kim, H., Boysen, D. A., Newhouse, J. M., Spatocco, B. L., Chung, B., Burke, P. J.. . Sadoway, D. R. (2013). Liquid metal batteries: Past, present, and future. *Chemical Reviews, 113*(3), 2075-2099. doi:10.1021/cr300205k

LaMonica, M. (2013). *A tiny startup called ambri wants to transform our energy system with massive liquid-metal batteries*. CAMBRIDGE: TECHNOL REV.

Linden, D. (1984). *Handbook of batteries and fuel cells*. New York: McGraw-Hill.

Martin, J. L., Zamora, I., Martin, J. I., Aperribay, V., & Eguia, P. (2011, April). Energy Storage Technologies for Electric Applications. Retrieved April 14, 2016, from http://www.sc.ehu.es/sbweb/energias-renovables/temas/almacenamiento/almacenamiento.html

Neburchilov, V., Wang, H., Martin, J. J., & Qu, W. (2010). A review on air cathodes for zinc–air fuel cells. *Journal of Power Sources, 195*(5), 1271-1291. doi:10.1016/j.jpowsour.2009.08.100

Otaegui, L., Rodriguez-Martinez, L. M., Wang, L., Laresgoiti, A., Tsukamoto, H., Han, M. H., & Rojo, T. (2014). Performance and stability of a liquid anode high-temperature metal air battery. Journal of Power Sources, 247, 749-755.

Palacios, I., Castillo, R., & Vargas, R. A. (2003). Thermal and transport properties of the polymer electrolyte based on poly(vinyl alcohol)-KOH-H2O.Electrochimica Acta, 48(14-16), 2195-2199. doi:10.1016/S0013-4686(03)00204-4

QuinteQ Energy Storage. (2014). Market for Energy Storage. Retrieved April 13, 2016, from http://www.quinteqenergy.com/market/

Schwenzer, B., Zhang, J., Kim, S., Li, L., Liu, J., & Yang, Z. (2011). Membrane development for vanadium redox flow batteries.*Chemsuschem, 4*(10), 1388-1406. doi:10.1002/cssc.201100068

Wang, H., & Turner, J. A. (2010). Reviewing metallic PEMFC bipolar plates. Fuel Cells, 10(4), 510-519. doi:10.1002/fuce.200900187

Wang, K., Jiang, K., Chung, B., Ouchi, T., Burke, P., Boysen, D.. . Sadoway, D. (2014). Lithium-antimony-lead liquid metal battery for grid-level energy storage.*Nature*, *514*(7522), 348-348. doi:10.1038/nature13700

Weber, A. Z., Mench, M. M., Meyers, J. P., Ross, P. N., Gostick, J. T., & Liu, Q. (2011). Redox flow batteries: A review.Journal of Applied Electrochemistry, 41(10), 1137-1164. doi:10.1007/s10800-011-0348-2

Young, W., Kuan, W., & Epps, T. H. (2013). Block copolymer electrolytes for rechargeable lithium batteries. *Journal of Polymer Science Part B: Polymer Physics J. Polym. Sci. Part B: Polym. Phys.*, *52*(1), 1-16. doi:10.1002/polb.23404

Zhang, J., et al., "A Metal-Free Bifunctional Electrocatalyst for Oxygen Reduction and Oxygen Evolution Reactions," *Nature Nanotechnology*, doi: 10.1038/nnano.2015.48 (Apr. 6, 2015).

Zhou, Ruolin. (2014). The Development of Zinc Air Battery's Efficiency and Rechargeability in Molten Alkaline Electrolyte. (Masters Research Report). Worcester Polytechnic Institute, Worcester, MA.

Appendix A: Anode Procedure with General Cell Assembly

The anode was prepared with liquid metal gallium as the active material and assembled by the following procedure:

1. **Liquid Metal Gallium Preparation**
    - 1.1. Cleaned all equipment with DI water
    - 1.2. Tared the stainless steel crucible inside the scale
    - 1.3. Set dram of solid gallium on a ring stand
    - 1.4. Applied heat to dram of gallium with heating lamp so it becomes a liquid
    - 1.5. Added liquid gallium to tared crucible until it measured approximately 1.2 g of gallium
2. **Teflon Gasket Preparation**
    - 2.1. Cut outer diameter of Teflon gasket using punch with 1.4 cm diameter
    - 2.2. Cut inner diameter of Teflon gasket using punch with 0.9 cm diameter
3. **Generally Cell Assembly**
    - 3.1. Set stainless steel anode collector into the bottom Teflon hexagonal Swagelok nut
    - 3.2. Set compression spring into anode collector
    - 3.3. Hand tightened middle Teflon hexagonal Swagelok union onto the bottom nut
    - 3.4. Set crucible with gallium inside middle union and on top of the spring using forceps
    - 3.5. Lay Teflon gasket on top of the crucible using forceps

Appendix B: Electrolyte Procedure with General Cell Assembly

Zirconia Cloth

The electrolyte layer constructed with zirconia material was wetted with 6M KOH and assembled by the following procedure:

1. **KOH Solution Preparation**
    1.1. Measured 10 mL of DI water in a graduated cylinder
    1.2. Tared 50 mL beaker inside scale
    1.3. Measured approximately 3.36 g of KOH
    1.4. Poured the 10 mL of DI water into beaker containing approximately 3.36 g of KOH
    1.5. Stirred until KOH was completely dissolved in the DI water
2. **Zirconia Cloth Separator Preparation**
    2.1. Cut 2 zirconia cloth separator with punch of diameter 1.1 cm
    2.2. Transferred cut zirconia cloth separators into beaker containing 6 M KOH using forceps
    2.3. Seal beaker with Parafilm
    2.4. Allowed separators to soak for approximately 20 minutes
3. **Gas Diffusion Layer Preparation**
    3.1. Cut platinum-catalyzed gas diffusion layer with a punch of diameter 1.1 cm
4. **General Cell Assembly**
    4.1. Removed separators from 6M KOH bath using forceps
    4.2. Placed one separator on top of the Teflon gasket using forceps
    4.3. Placed second separator on top of the first separator using forceps
    4.4. Placed platinum-catalyzed gas diffusion layer on top of second separator with forceps

Appendix C: Cathode Procedure with General Cell Assembly

The air cathode is prepared and assembled using the following procedure:

1. **Air Cathode Preparation**

    1.1. Fit 1 Teflon gaskets, with the outer diameter of 1.4 cm and inner diameter of 0.9 cm, onto stainless steel cathode current collector

    1.2. Fit air cathode current collector with gaskets into top Teflon hexagonal Swagelok nut

    1.3. Hand tightened top nut onto middle union, pressing in the cathode current collector for a better seal

Appendix D: Structural Assembly and Software Implementation

1. Structural Assembly

1.1. Invert cell so cathode is pointing downwards

1.2. Tighten cell midway onto a ring clamp on a ring stand under a heat lamp

1.3. Attach temperature probe to the ring clamp to measure ambient temperature approximately around the middle of the cell

2. Software Implementation

2.1. Load premade script, depending on which test is being run, as the program

2.2. Wait until temperature reading stabilizes at desired temperature

2.3. Adjust ring clamp and cell height if temperature is not at desired point

2.4. Run program

Appendix E: Cell Assembly Process

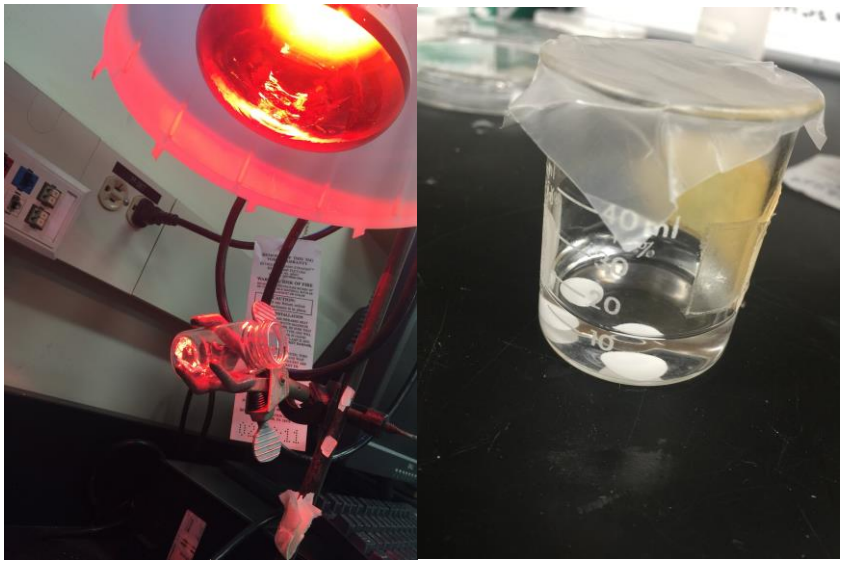

Figure 38: Heating gallium in glass vial (left). Soaking separators in KOH (right).

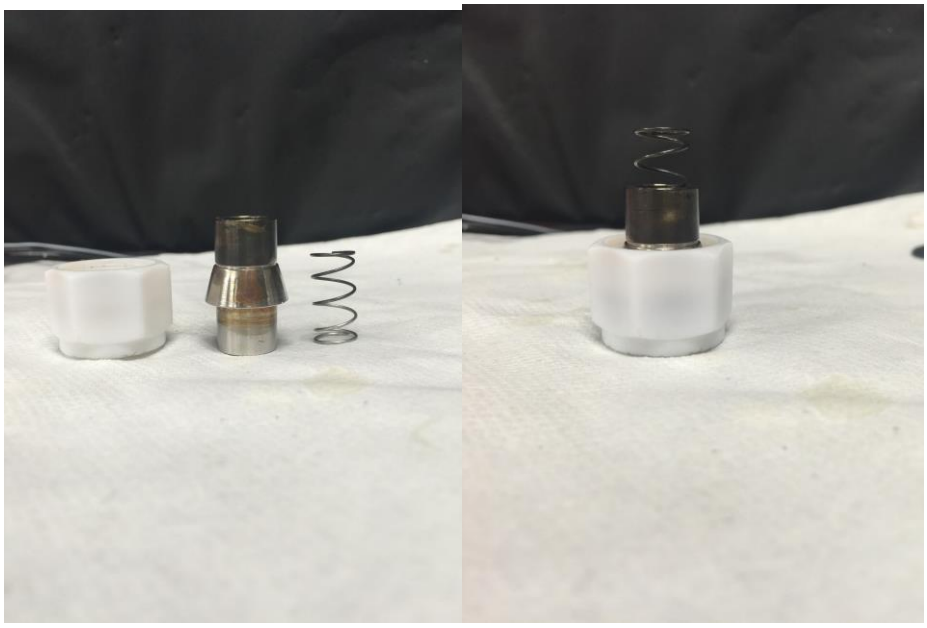

Figure 39: Anode Assembly

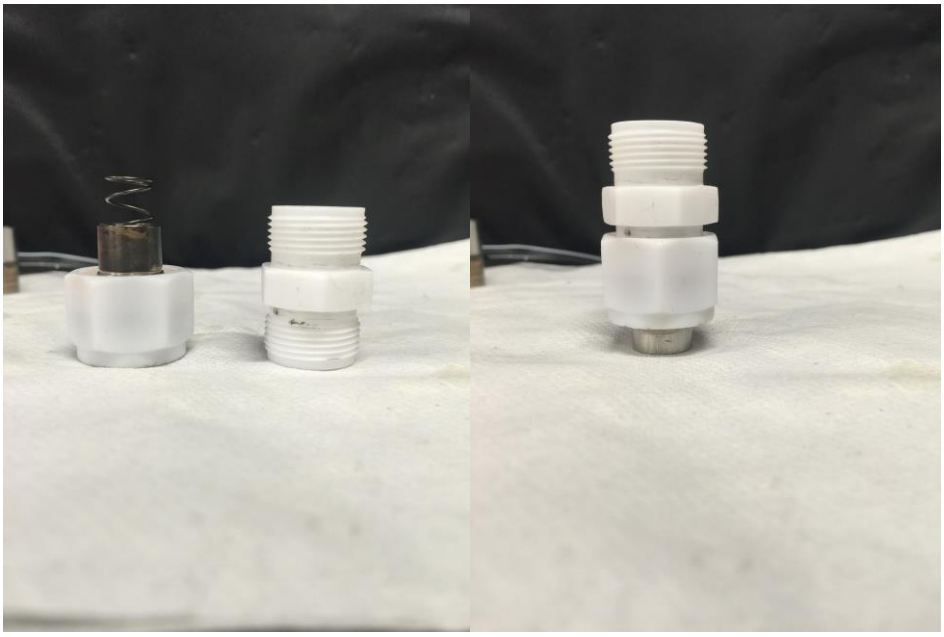

Figure 40: Anode assembly (continued)

Figure 41: Gallium measurement process

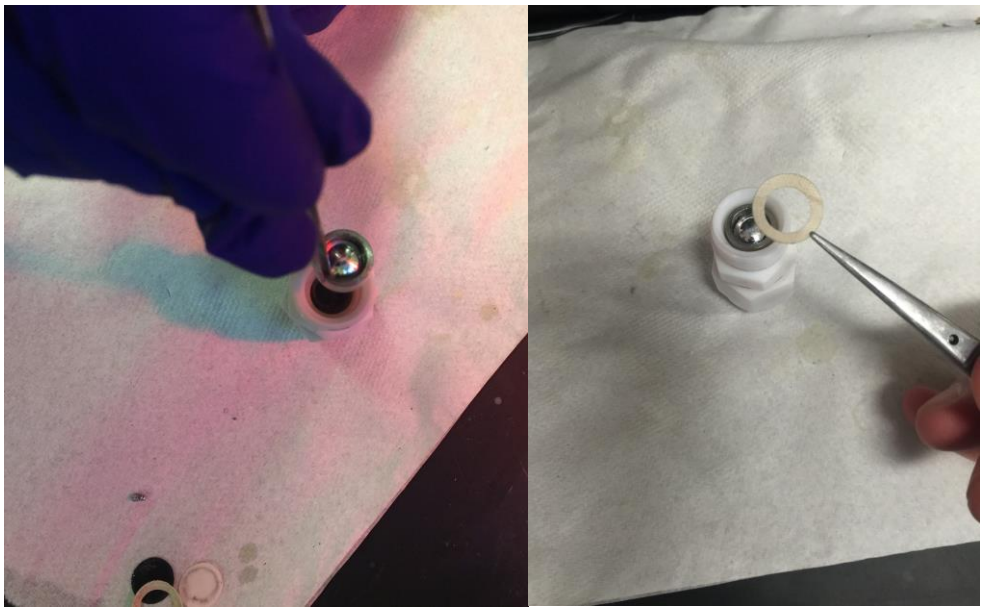

Figure 42: Crucible and gasket assembly

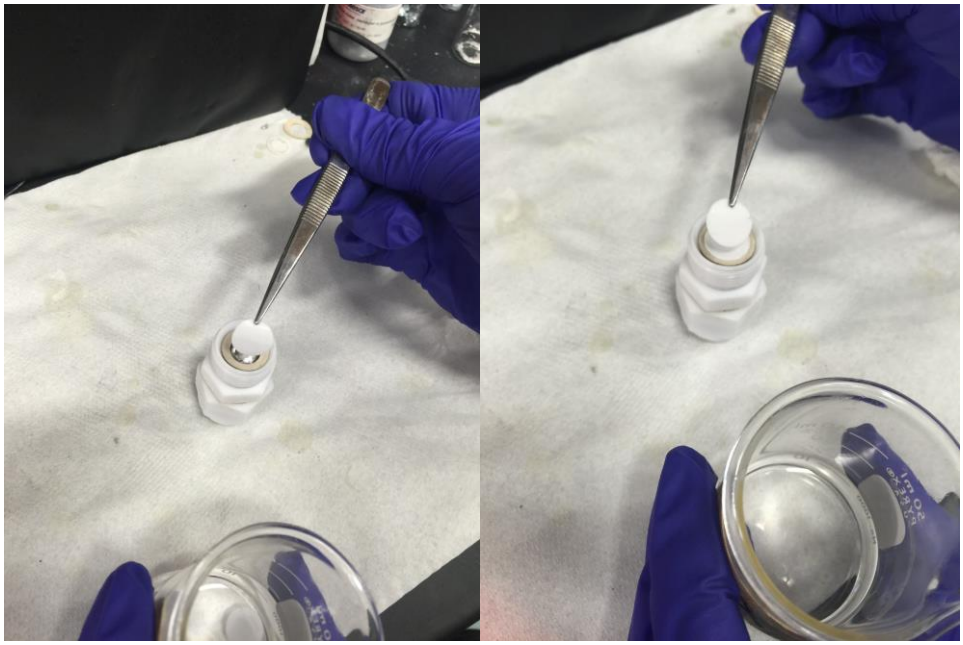

Figure 43: Two separator assembly

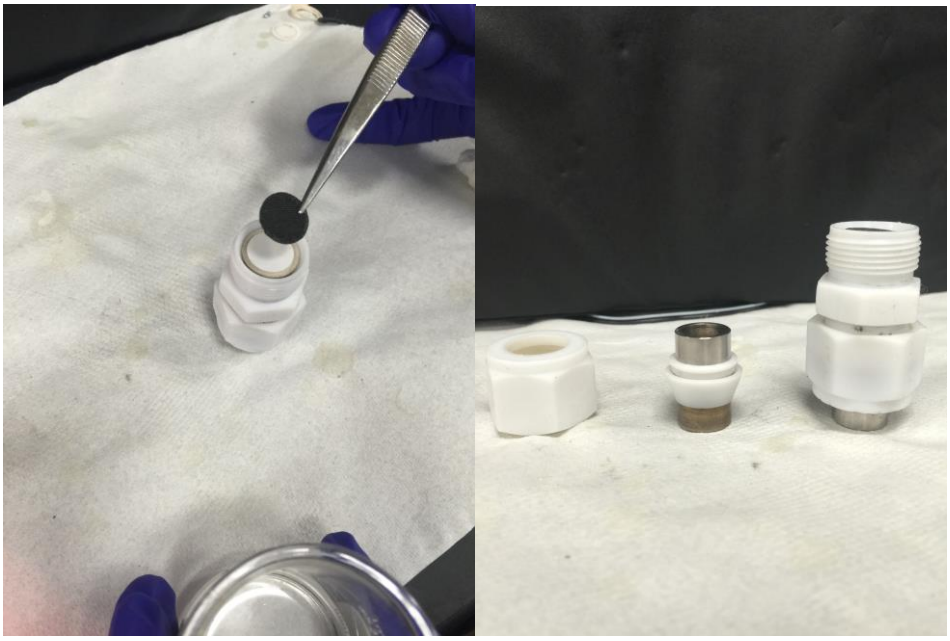

Figure 44: GDL and cathode assembly

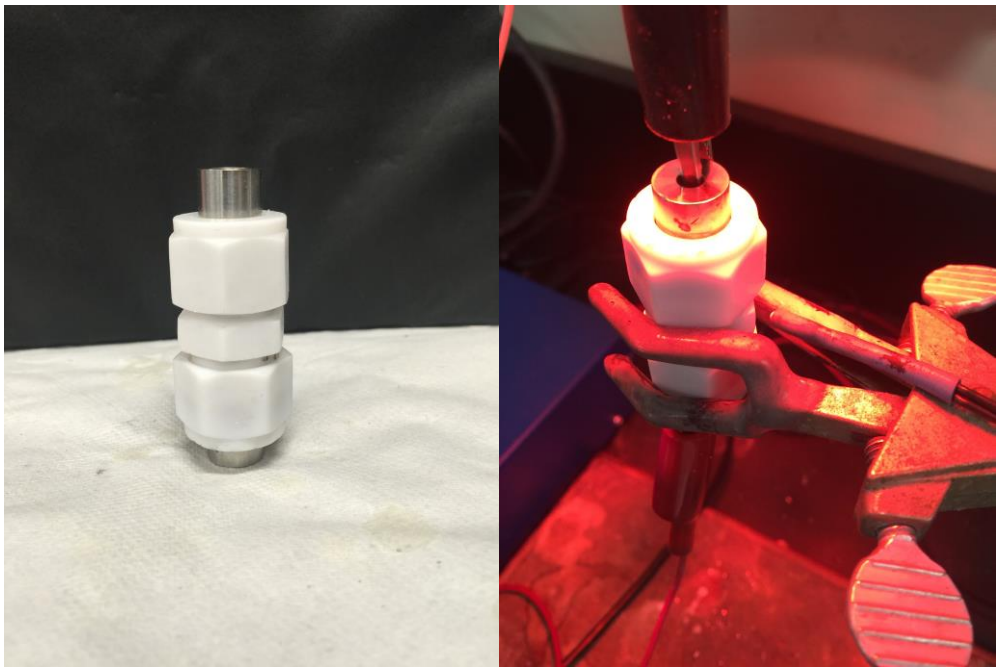

Figure 45: Completed cell (left). Inverted ring stand assembly (right)